NASA CONTRACTOR REPORT

NASA CR-1909

EXPERIMENTAL STUDY OF ROTOR UNSTEADY AIRLOADS DUE TO BLADE-VORTEX INTERACTION

by Raghuveera Padakannaya

Prepared by
THE PENNSYLVANIA STATE UNIVERSITY
University Park, Pa.
for Langley Research Center

NATIONAL AERONAUTICS AND SPACE ADMINISTRATION • WASHINGTON, D. C. • NOVEMBER 1971

1. Report No.	2. Government Accession No.	3. Recipient's Catalog No.
NASA CR-1909		

4. Title and Subtitle	5. Report Date
EXPERIMENTAL STUDY OF ROTOR UNSTEADY AIRLOADS DUE TO BLADE-VORTEX INTERACTION	November 1971
	6. Performing Organization Code
7. Author(s)	8. Performing Organization Report No.
Raghuveera Padakannaya	PSU AERSP 71-1
	10. Work Unit No.
9. Performing Organization Name and Address	
The Pennsylvania State University University Park, Pennsylvania	11. Contract or Grant No. NGR-39-009-111
	13. Type of Report and Period Covered Contractor Report
12. Sponsoring Agency Name and Address	
National Aeronautics and Space Administration Washington, D.C. 20546	14. Sponsoring Agency Code

15. Supplementary Notes

This report supplements NASA CR-1573.

16. Abstract

Additional measurements of unsteady, rotor-blade airloads and their time derivatives are presented for a rotor blade intersecting a completely rolled-up vortex. These results, taken at the blade spanwise station of 0.9R, 0.85R, and 0.75R, complement measurements previously reported for the 0.95R station in CR-1573. Incremental values in the section lift coefficient as high as 1.17 were obtained at the 0.75R station. Generally, these values decreased with increasing radius.

17. Key Words (Suggested by Author(s))	18. Distribution Statement
Helicopter airloads Unsteady aerodynamics Vortex flow	Unclassified - Unlimited

19. Security Classif. (of this report)	20. Security Classif. (of this page)	21. No. of Pages	22. Price*
Unclassified	Unclassified	38	$3.00

*For sale by the National Technical Information Service, Springfield, Virginia 22151

NOMENCLATURE

c	Blade chord
C_l	Section lift coefficient based on the local rotational velocity, ωr
h	Radial distance from the center of the vortex
r	Radius at any spanwise station from the center of rotation
R	Blade radius
t	Time
V	Free stream velocity
V_T	Blade tip velocity
Z	Distance between rotor axis and vortex axis
α_w	Vortex generated wing angle of attack
Γ	Circulation at any radius
Δ	Denotes increment in a quantity
δ	Intersection angle
μ	Advance ratio = $V/\omega R$

SUMMARY

Additional measurements of unsteady, rotor blade airloads and their time derivatives are presented for a rotor blade intersecting a completely rolled-up vortex. These results, taken at the spanwise stations of 0.9R, 0.85R and 0.75R complement measurements previously reported for the 0.95R station.

Incremental values in the section lift coefficient as high as 1.17 were obtained at the 0.75R station. Generally, these values decreased with increasing radius.

INTRODUCTION

The intersection of a rotor blade with the tip vortex from a preceding blade can result in an appreciable impulsive load near the blade tip producing structural vibrations and the sharp, cracking sound known as blade slap or bang. This investigation of the rotor vortex interaction utilizes a flat-pitched rotor blade with a symmetrical airfoil section. The rotor disc plane, also at a zero angle of attack, intersects a completely rolled-up vortex generated by a fixed wing ahead of the plane. Time histories of the chordwise pressure distribution are recorded at three spanwise locations of the blade for two different RPMs and for different rotor plane positions and angle of intersections.

This report represents an extension of the work reported in Reference 1. The reader is referred to the reference for a more complete description of the test apparatus and procedures.

DESCRIPTION OF EXPERIMENT

The experimental equipment can be positioned vertically and horizontally so that the blade intersects the vortex system at different orientations. The single, instrumented blade, made of high strength aluminum, used for the tests was one foot in radius, two inches in chord with an NACA 0015 airfoil section. The miniature pressure sensors, placed in the grooves, were flush with the surface of the blade. Electrical lead wires followed along the spanwise grooves on the blade through the shaft to a slip ring unit.

The experiments were conducted in the subsonic wind-tunnel of the Department of Aerospace Engineering at The Pennsylvania State University using an open-jet test section. The vortex-generating wing, mounted vertically at the end of the contraction section of the wind-tunnel, generated a vortex of 15.25ft.^{2}/sec strength at 10° angle of attack. Since the blade is instrumented only on one surface, to get the pressure distribution on the other surface the direction of the vortex rotation is changed by changing the angle of attack of the wing from positive to negative.

The ultraminiature pressure sensors used in this experiment were 1/8" in diameter and 0.02" thick with a natural frequency of 40kc and a sensitivity of approximately 0.75 mV/V/psi with a range of 0-25 psi. The RPM of the rotor was measured accurately through an electronic counter. A triggering mechanism was used to obtain the results during the short time that the blade passes through the vortex.

The rotor and the vortex-generating wing in the wind-tunnel are shown in Figure 1. A test velocity of 75 mph was used for all the testing. After establishing the test velocity the reference station for the vertical movement of the shaft was formed by moving the shaft such that the vortex axis and shaft axis lay on a horizontal plane. After a warming up period, the output of the sensors were individually balanced.

Measurements were conducted for four vertical locations of the shaft axis (i.e. Z/R = 0; 0.25; 0.5 and 0.75), four to five locations of the rotor plane (i.e.) h/c = -1.0 to 1.0, two rotational speeds and three spanwise stations. The scope traces of the pressure transducers were recorded photographically to obtain timewise variation of the pressures measured by the chordwise pressure sensors. The photographs were read using a trace reader with the results being recorded on IBM cards. These were matched with the corresponding results of the pressures on the other surface of the blade and processed through an IBM 360/67 computer.

PRESENTATION OF RESULTS

The maximum lift difference and its time variation as the blade intersects the vortex are important for the estimation of the unsteady blade stresses and for the intensity of the resulting noise. The variations of ΔC_l and $\Delta C_l/\Delta t$ with rotor plane position, h/c, for the two values of RPM's, 1500 and 2000, for the three spanwise stations, 0.9R, 0.85R and 0.75R, are shown in Figures 2, 3, 4, 5, 7, 8, 9, 10, 12, 13, 14, 15 and 16. The general variations of ΔC_l and $\Delta C_l/\Delta t$ with h/c are similar. All the peak values of ΔC_l and $\Delta C_l/\Delta t$ occur at or near the center. The results presented in this report and those presented in Reference 1 show that at a given Z/R and RPM, the maximum lift coefficient difference, ΔC_l, at the inboard span stations are greater than those at the outboard span stations. Though the values of ΔC_l for the 2000 RPM case are smaller than those for the case of 1500 RPM under similar conditions, the actual lift increments will be greater due to the higher velocity. As observed in Reference 1 the maximum lift coefficient difference, ΔC_l, increases with increasing Z/R (decreasing intersection angles) at a given spanwise station.

The effect of vortex strength on the parameter ΔC_l and $\Delta C_l/\Delta t$ is shown in Figures 6, 11 and 17 for the case of Z/R = 0 and for different rotor plane positions (h/c) for the three spanwise stations 0.9R, 0.85R and 0.75R. The vortex strengths are non-dimensionalized with tip velocity and blade radius. Both the parameters appear to increase linearly with vortex strength, the rate of increase being dependent on (h/c). The maximum increase occurs when the blade passes through

the center of the vortex. The variations of ΔC_l and $\frac{\Delta C_l}{\Delta t}$ along the span of the blade are shown for 1500 RPM and different h/c values in Figures 18, 19, 20, 21, 22, 23, 24 and 25 for Z/R values of 0, 0.25, 0.5 and 0.75. Figures 26 and 27 show typical variations of ΔC_l and $\frac{\Delta C_l}{\Delta t}$ for Z/R = 0 at 2000 RPM. The plots of ΔC_l and $\frac{\Delta C_l}{\Delta t}$ for other values of Z/R at 2000 RPM can be obtained by cross plotting the results shown in Figures 3, 4, 5, 8, 9, 10, 14, 15 and 16. The ΔC_l values appear to decrease towards the tip of the blade. But $\frac{\Delta C_l}{\Delta t}$ does not exhibit a consistent variation along the span.

CONCLUSIONS

Additional results of an experimental investigation of rotor blade-vortex interaction have been presented. The conclusions to be drawn from the results are as follows:

1. The maximum lift coefficient difference, ΔC_l, and their time variations are a maximum when the rotor intersects the center of the vortex.
2. Values of ΔC_l as high as 1.15 at 0.75R and 0.75 x 10^3/sec for $\frac{\Delta C_l}{\Delta t}$ at 0.9R were measured in the present experiments.
3. ΔC_l and $\frac{\Delta C_l}{\Delta t}$ increase approximately linearly with vortex strength with the slopes being different for different rotor plane positions.
4. ΔC_l at each span station increases as the shaft axis is moved away from the vortex axis (i.e. as the intersection angle decreases)
5. At a particular Z/R, ΔC_l at the inboard span stations are higher than those at the outboard span stations. However, no definite trend exists in the case of the time variation of maximum lift difference ; i.e., $\frac{\Delta C_l}{\Delta t}$

REFERENCE

1. Surendraiah, M., An Experimental Study of Rotor Blade-Vortex Interaction, M.S. Thesis, The Pennsylvania State University, 1969; (Also published as NASA CR-1573, May 1970)

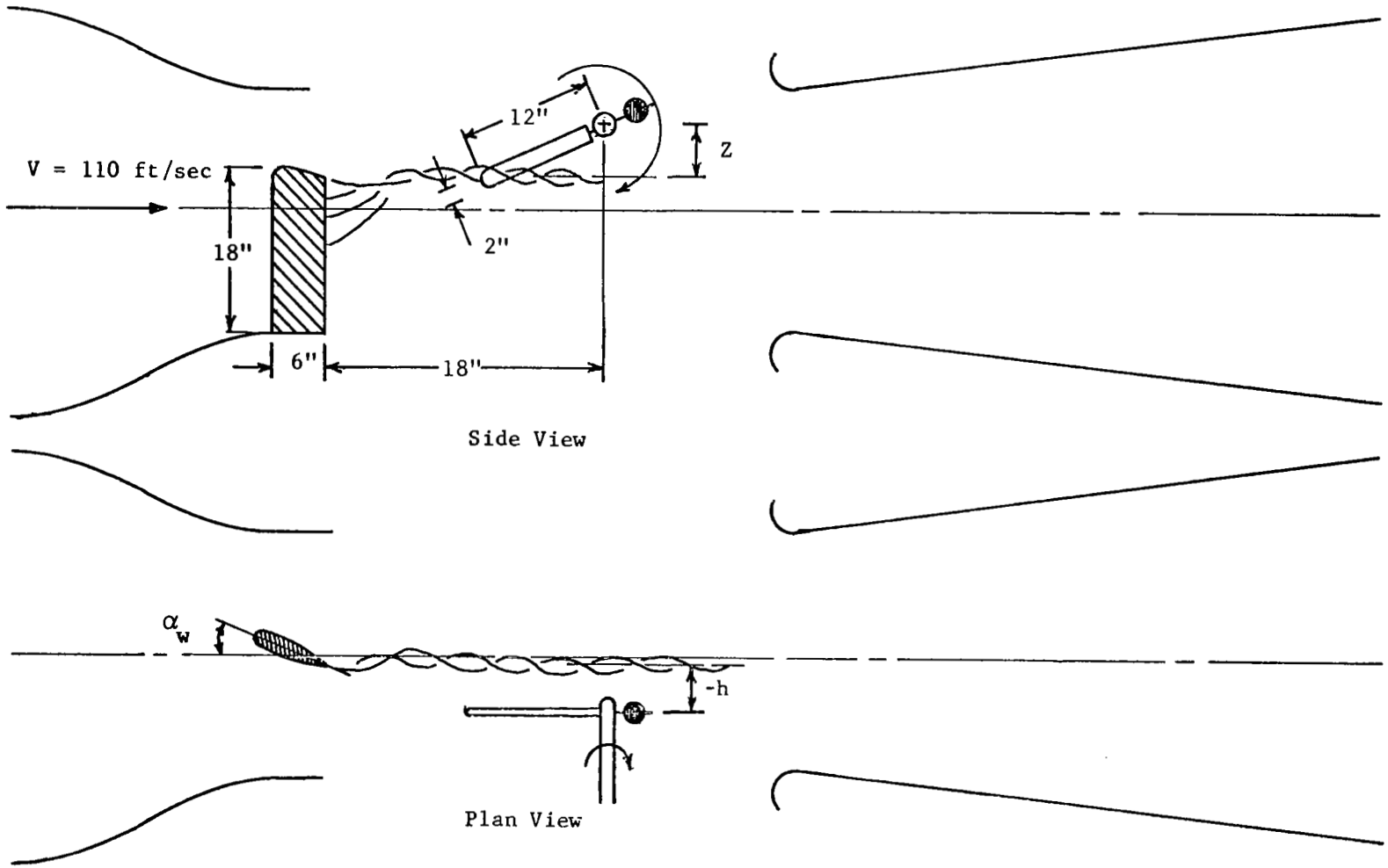

Fig. 1 Schematic Layout of the Test Set-Up in the Wind-Tunnel

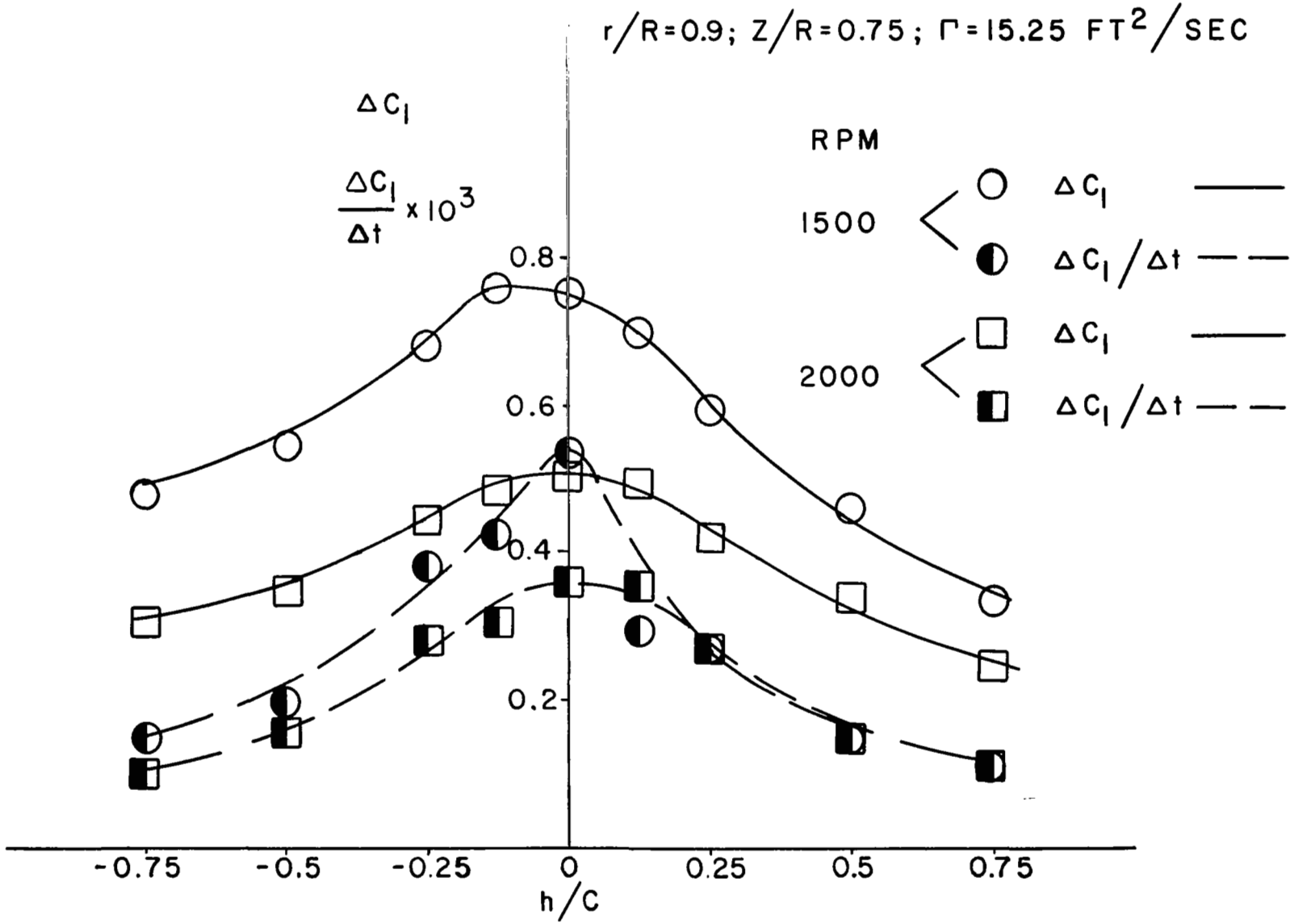

Fig. 2 Variation of ΔC_l and $\frac{\Delta C_l}{\Delta t}$ with Rotor Plane Positions

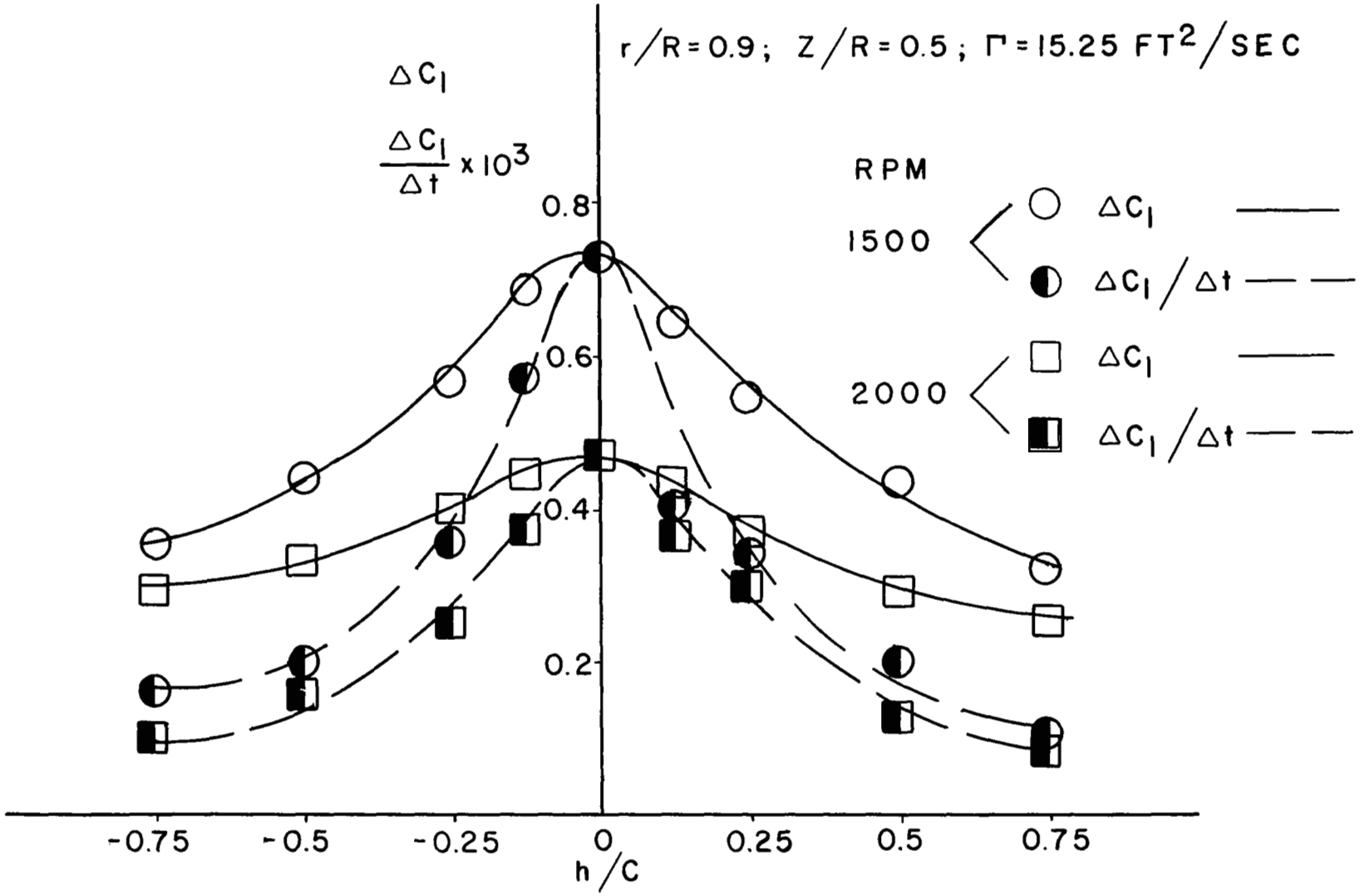

Fig. 3 Variation of ΔC_l and $\frac{\Delta C_l}{\Delta t}$ with Rotor Plane Positions

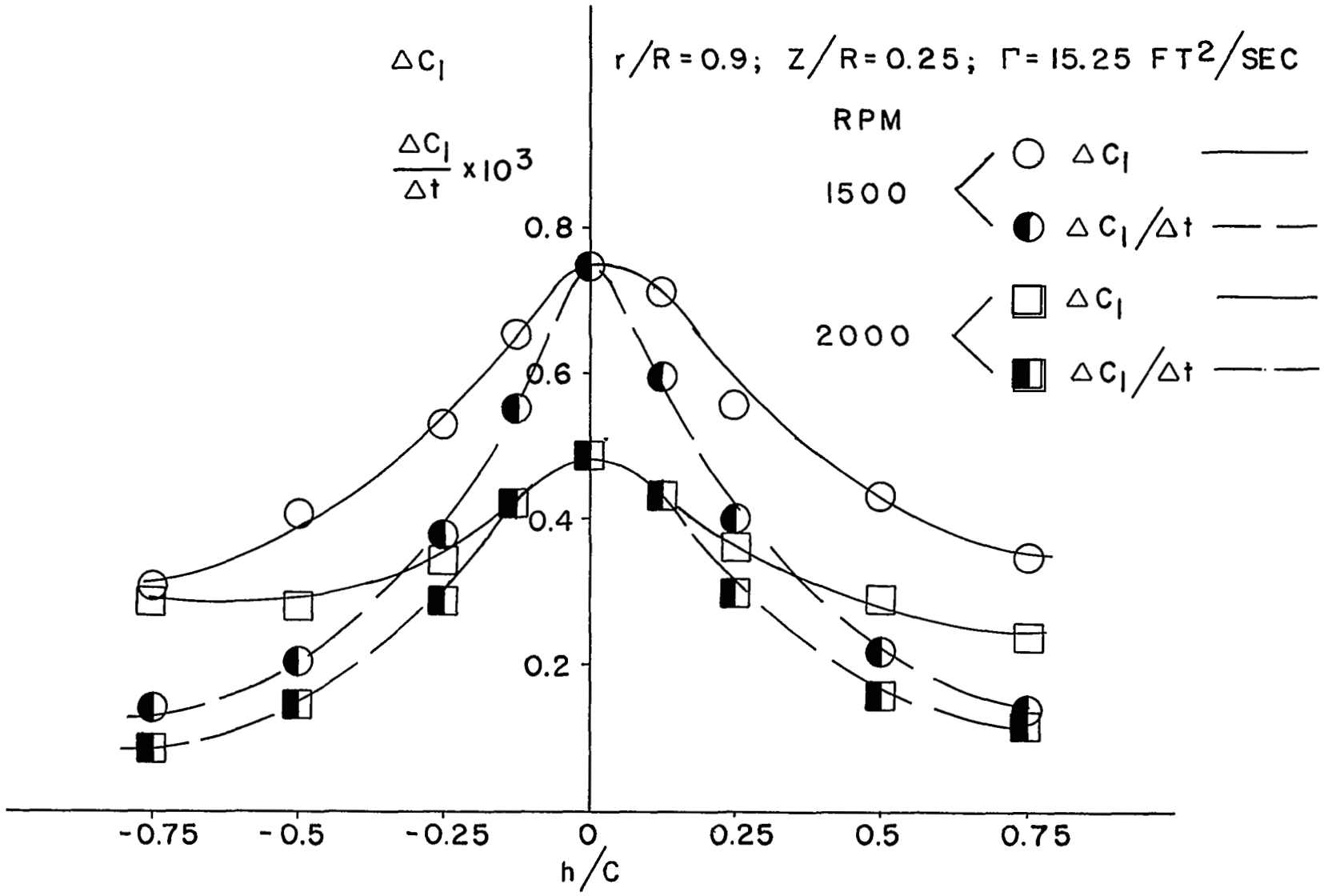

Fig. 4 Variation of ΔC_l and $\frac{\Delta C_l}{\Delta t}$ with Rotor Plane Positions

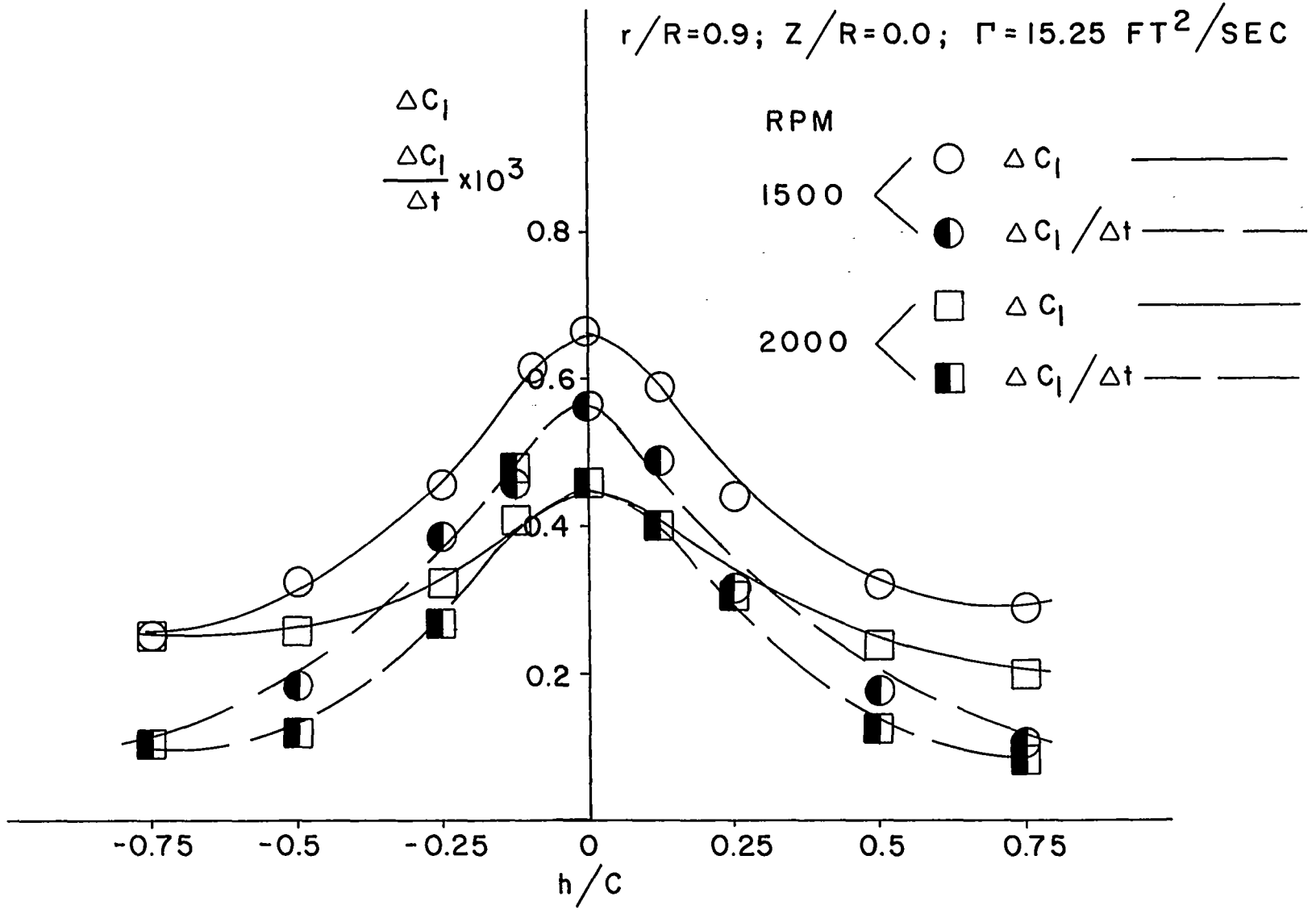

Fig. 5 Variation of ΔC_l and $\frac{\Delta C_l}{\Delta t}$ with Rotor Plane Positions

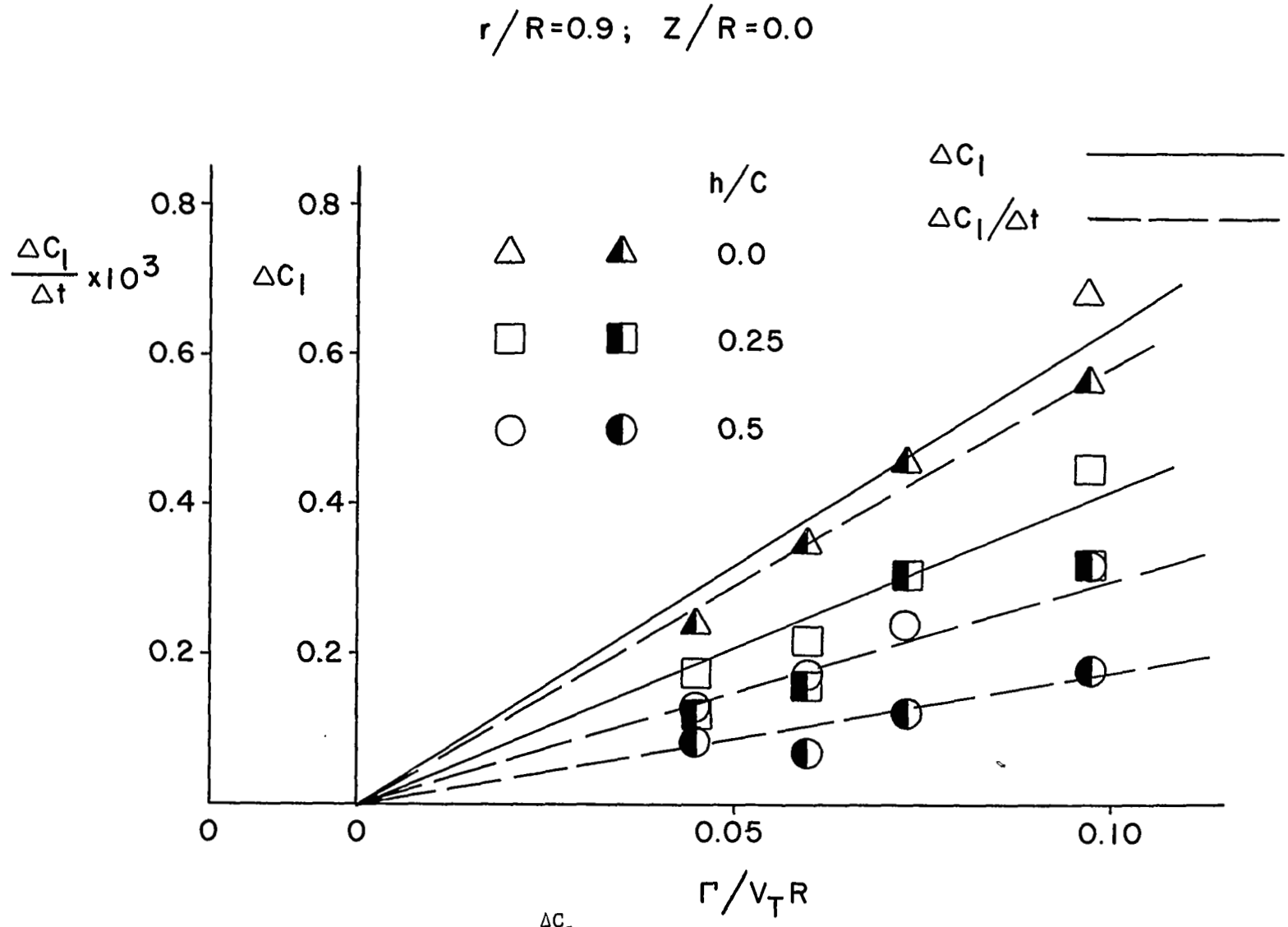

Fig. 6 Variation of ΔC_l and $\frac{\Delta C_l}{\Delta t}$ with Circulation

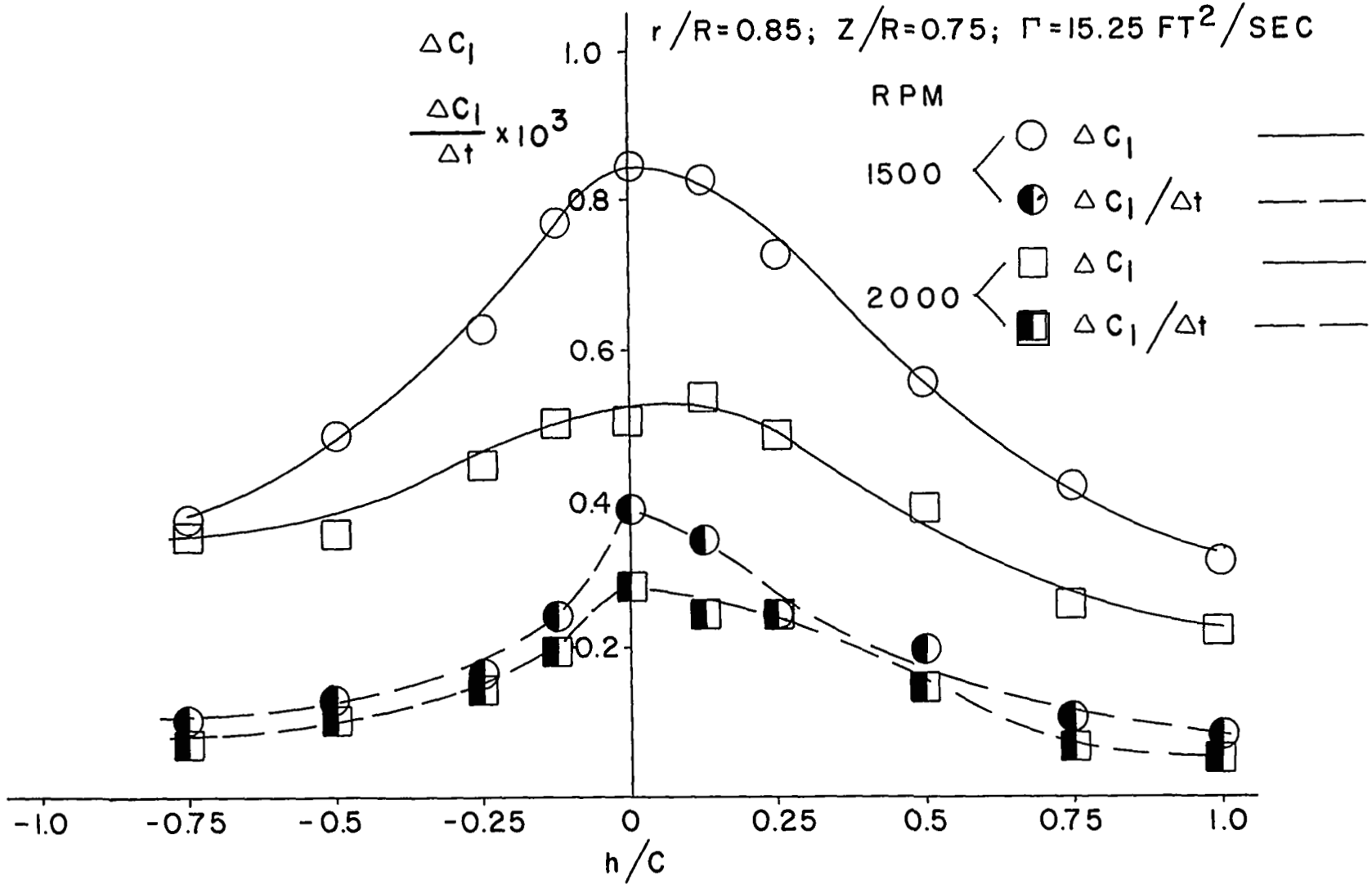

Fig. 7 Variation of ΔC_l and $\frac{\Delta C_l}{\Delta t}$ with Rotor Plane Positions

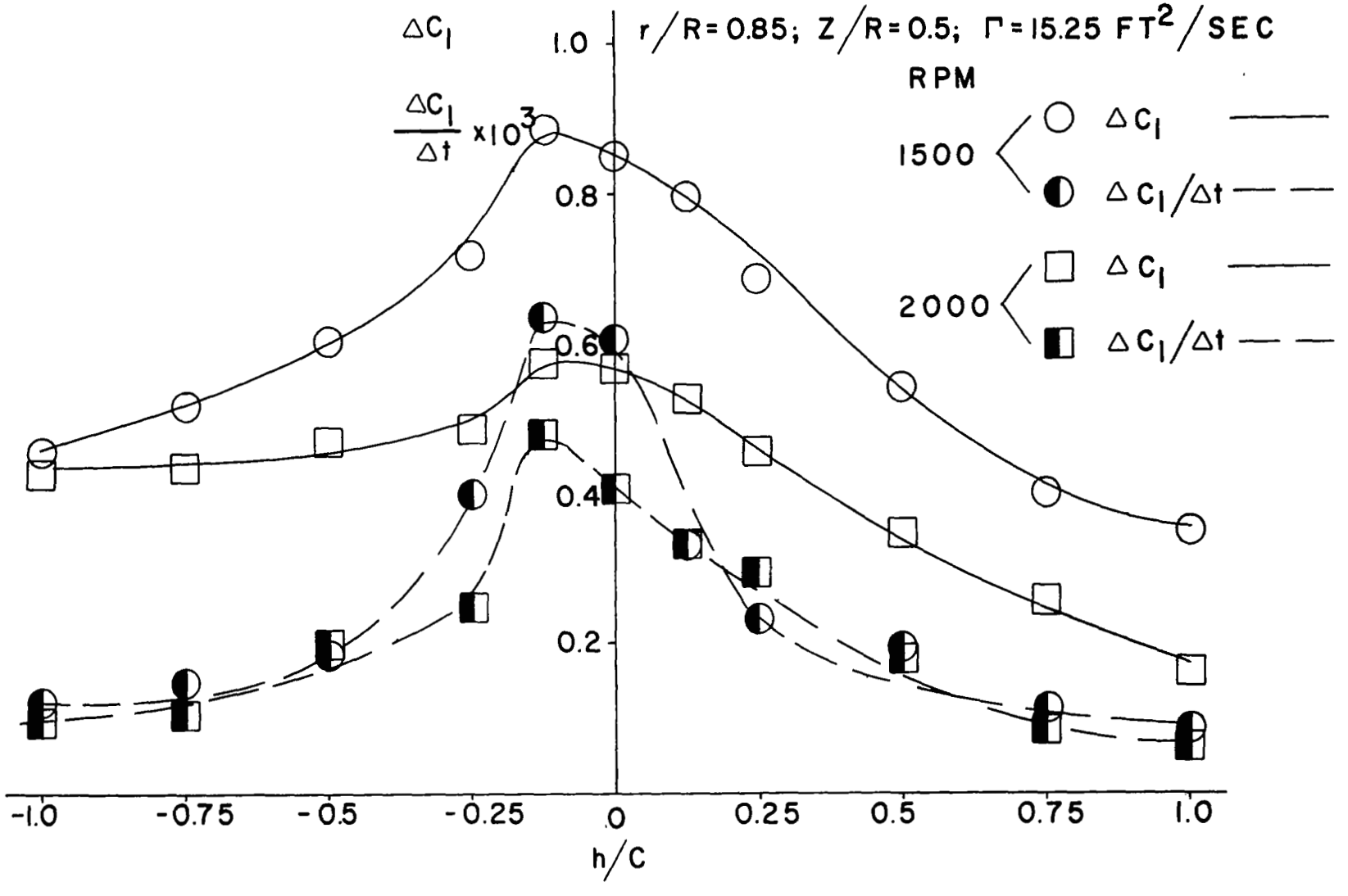

Fig. 8 Variation of ΔC_l and $\frac{\Delta C_l}{\Delta t}$ with Rotor Plane Positions

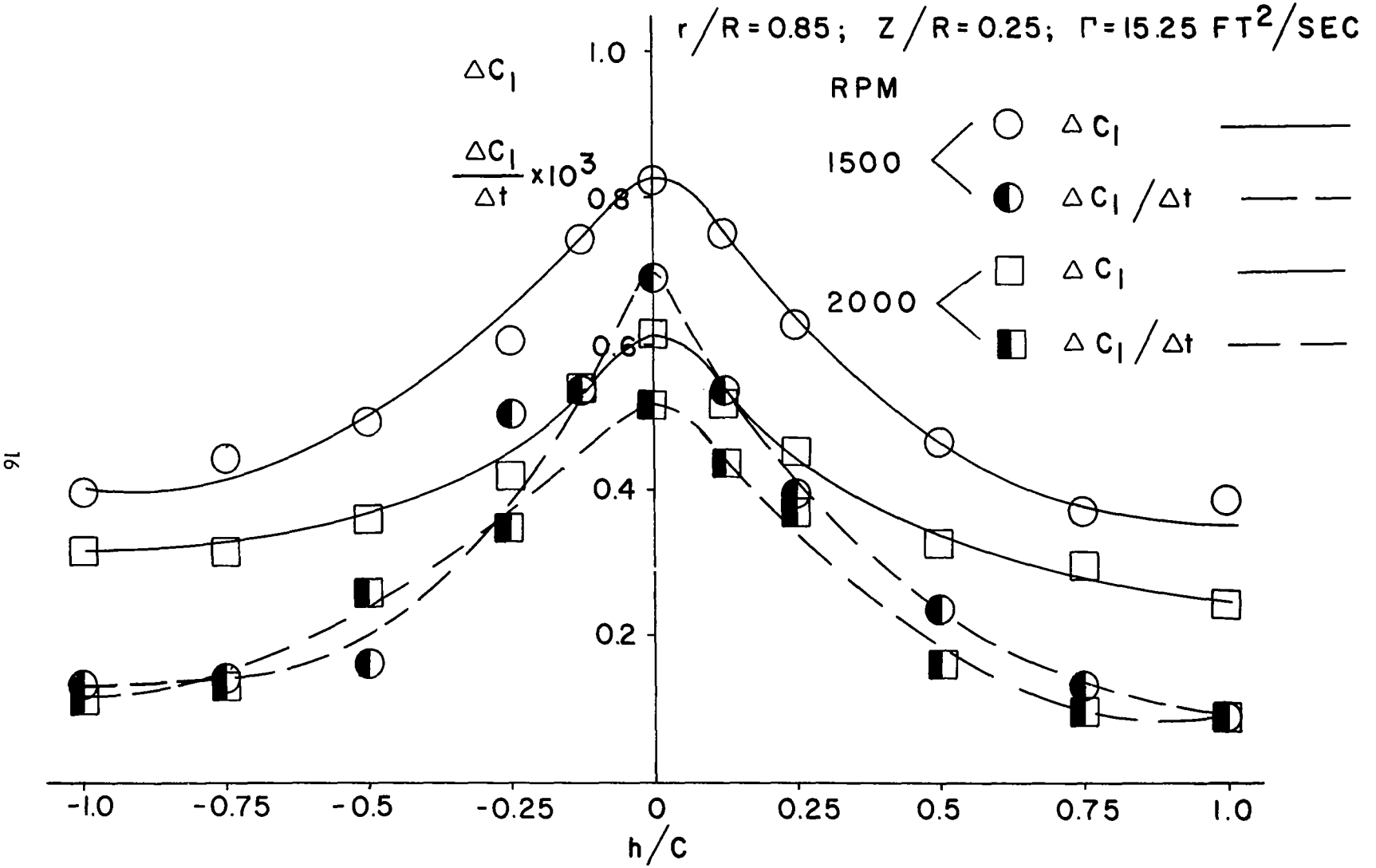

Fig. 9 Variation of ΔC_l and $\frac{\Delta C_l}{\Delta t}$ with Rotor Plane Positions

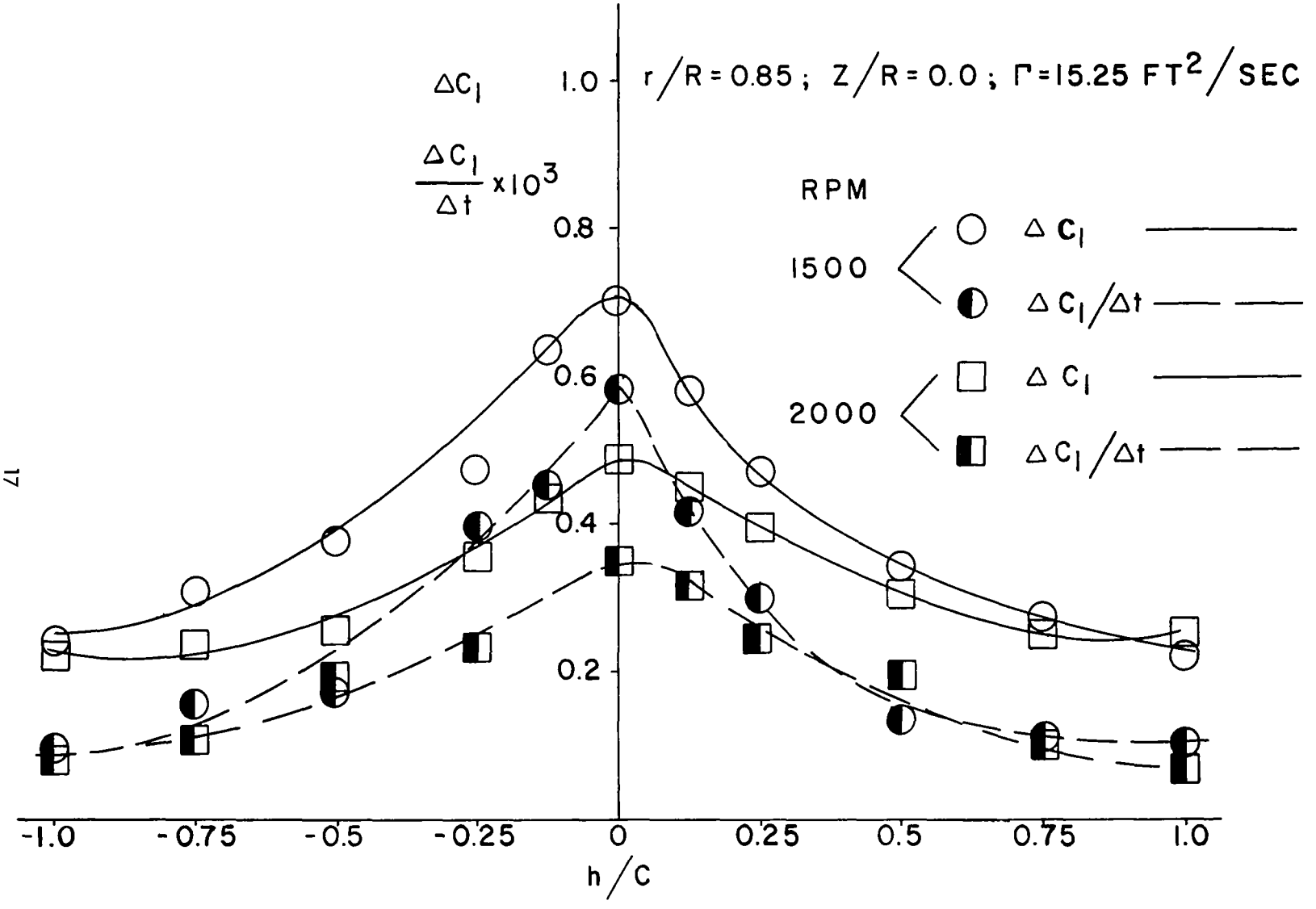

Fig. 10 Variation of ΔC_l and $\frac{\Delta C_l}{\Delta t}$ with Rotor Plane Positions

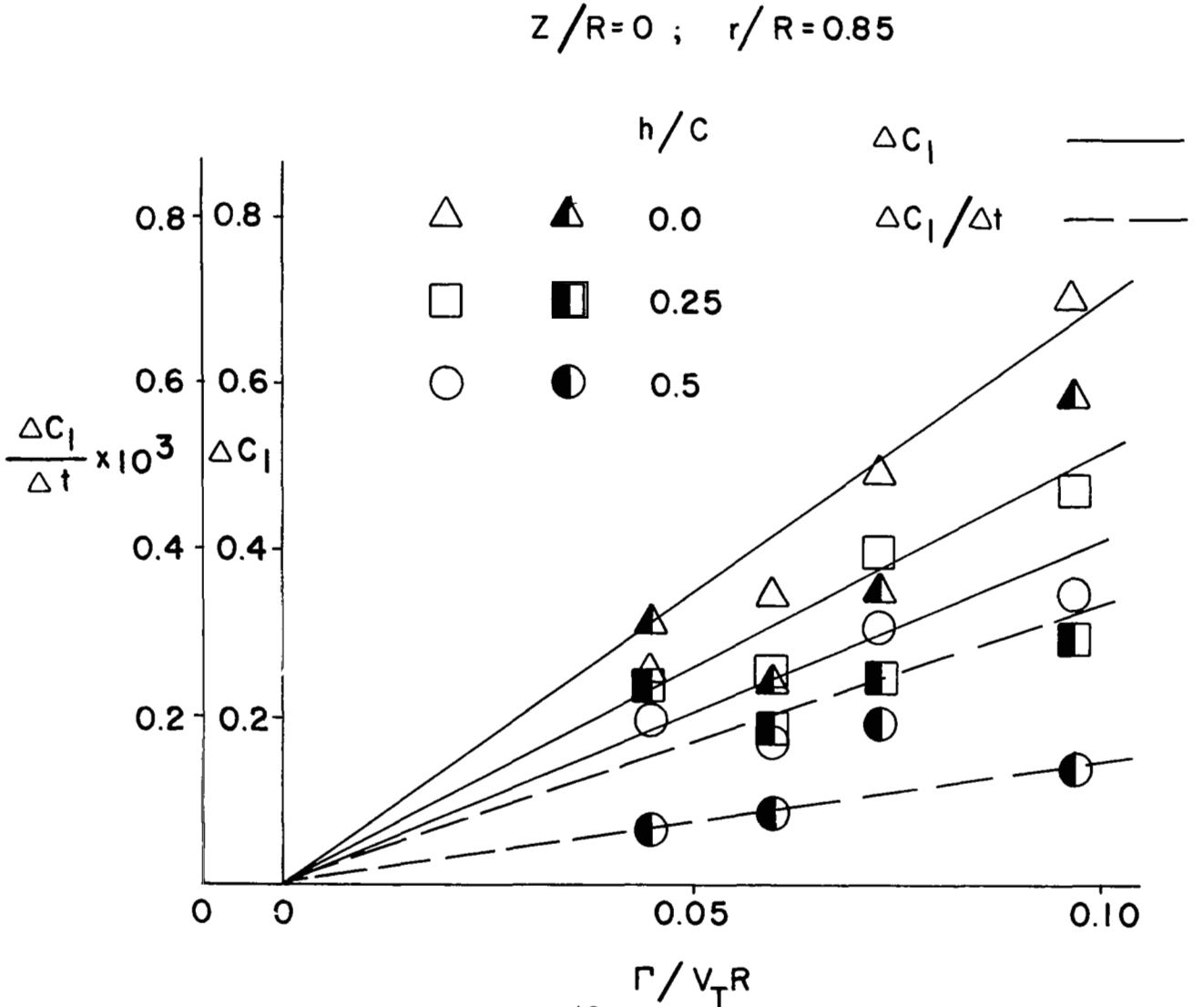

Fig. 11 Variation of ΔC_l and $\frac{\Delta C_l}{\Delta t}$ with Circulation

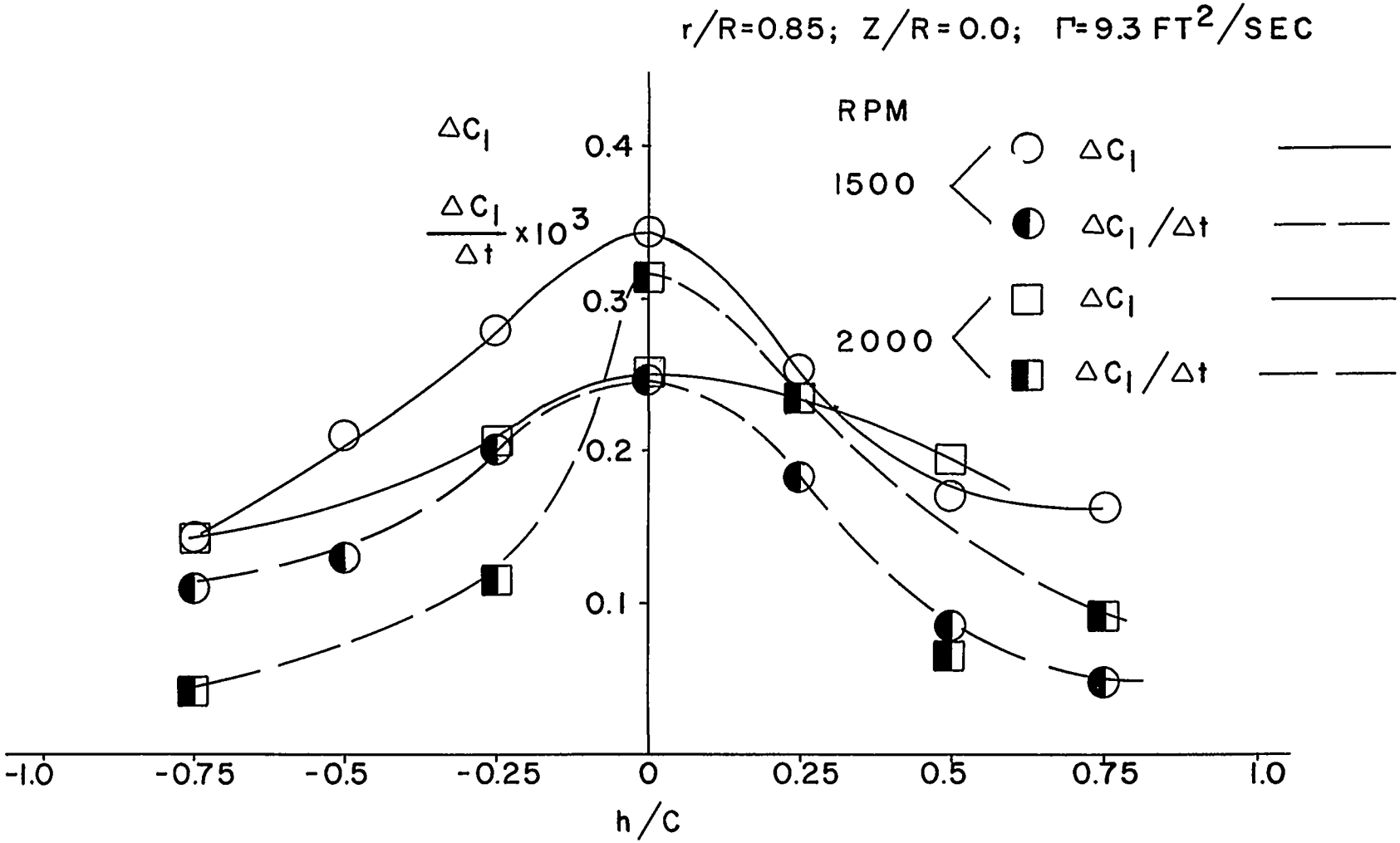

Fig. 12 Variation of ΔC_l and $\frac{\Delta C_l}{\Delta t}$ with Rotor Plane Positions

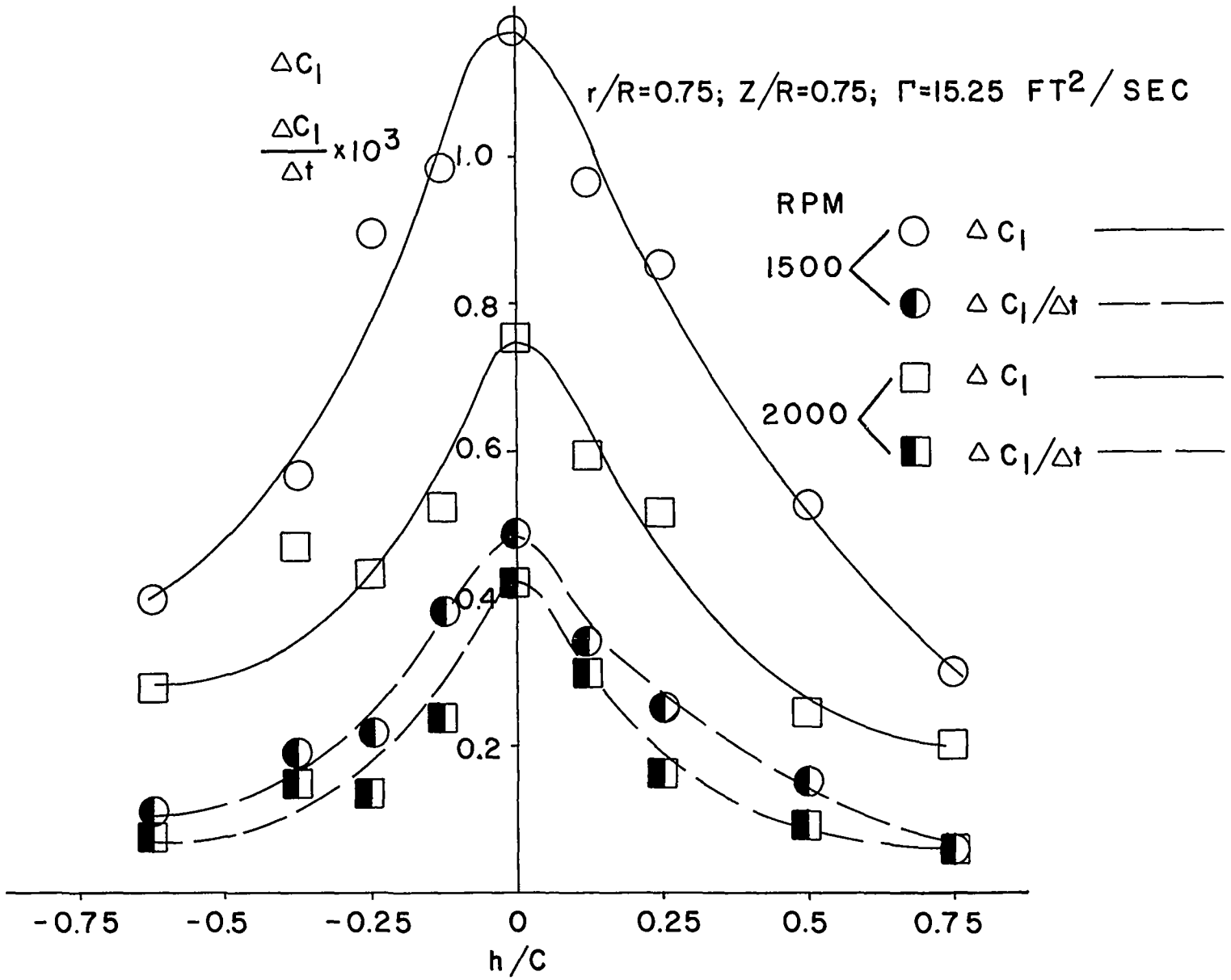

Fig. 13 Variation of ΔC_1 and $\frac{\Delta C_1}{\Delta t}$ with Rotor Plane Positions

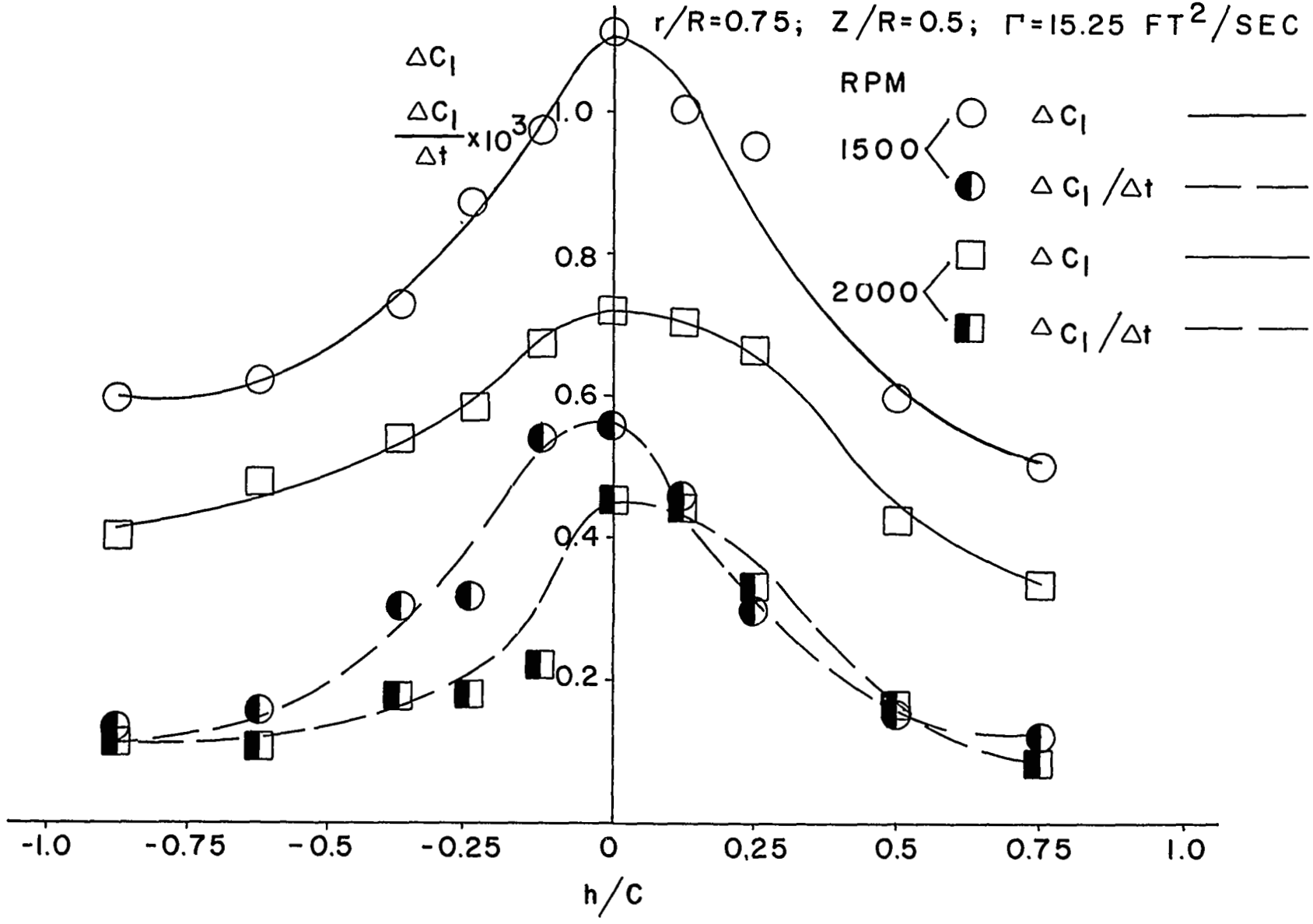

Fig. 14 Variation of ΔC_1 and $\frac{\Delta C_1}{\Delta t}$ with Rotor Positions

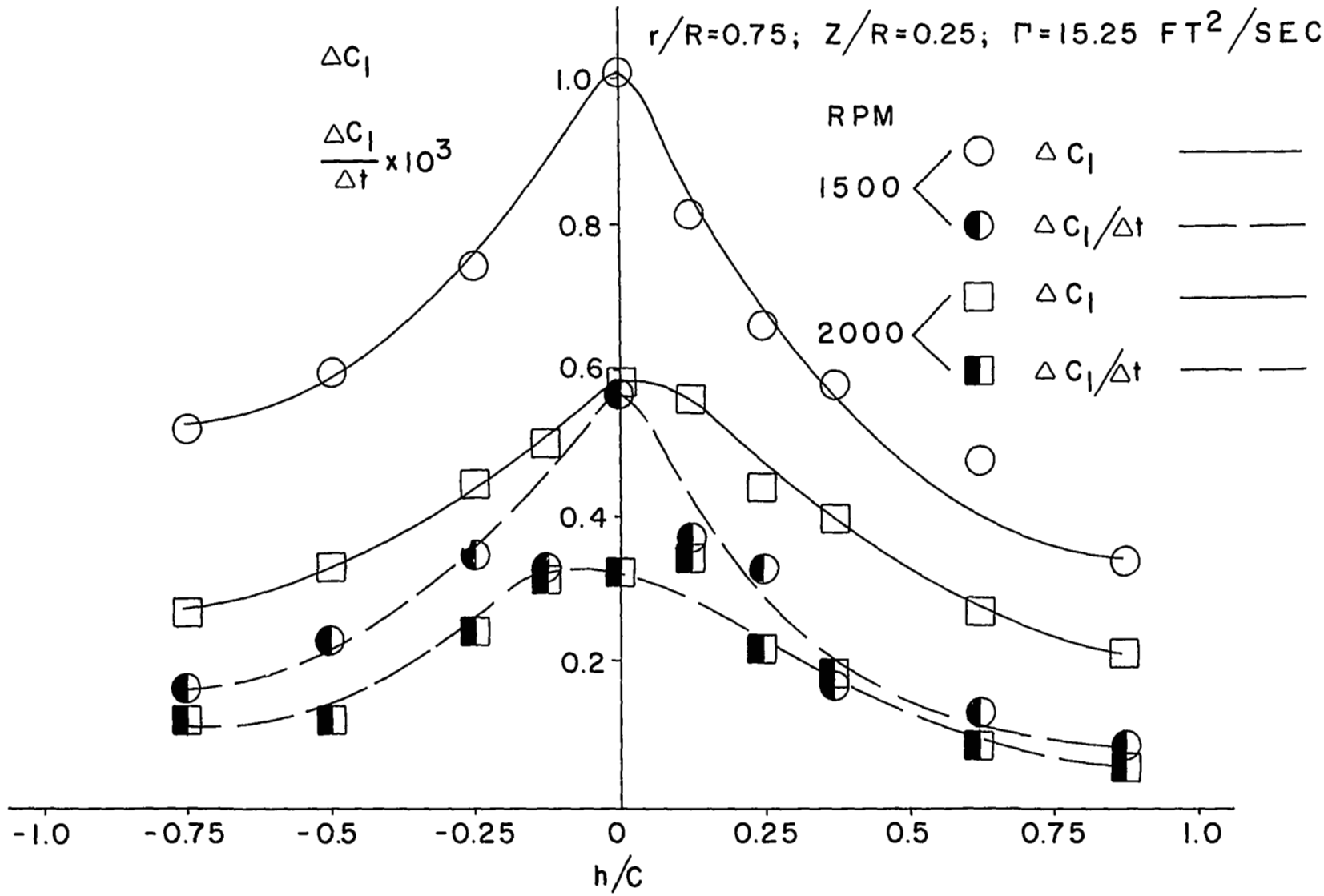

Fig. 15 Variation of ΔC_l and $\frac{\Delta C_l}{\Delta t}$ with Rotor Positions

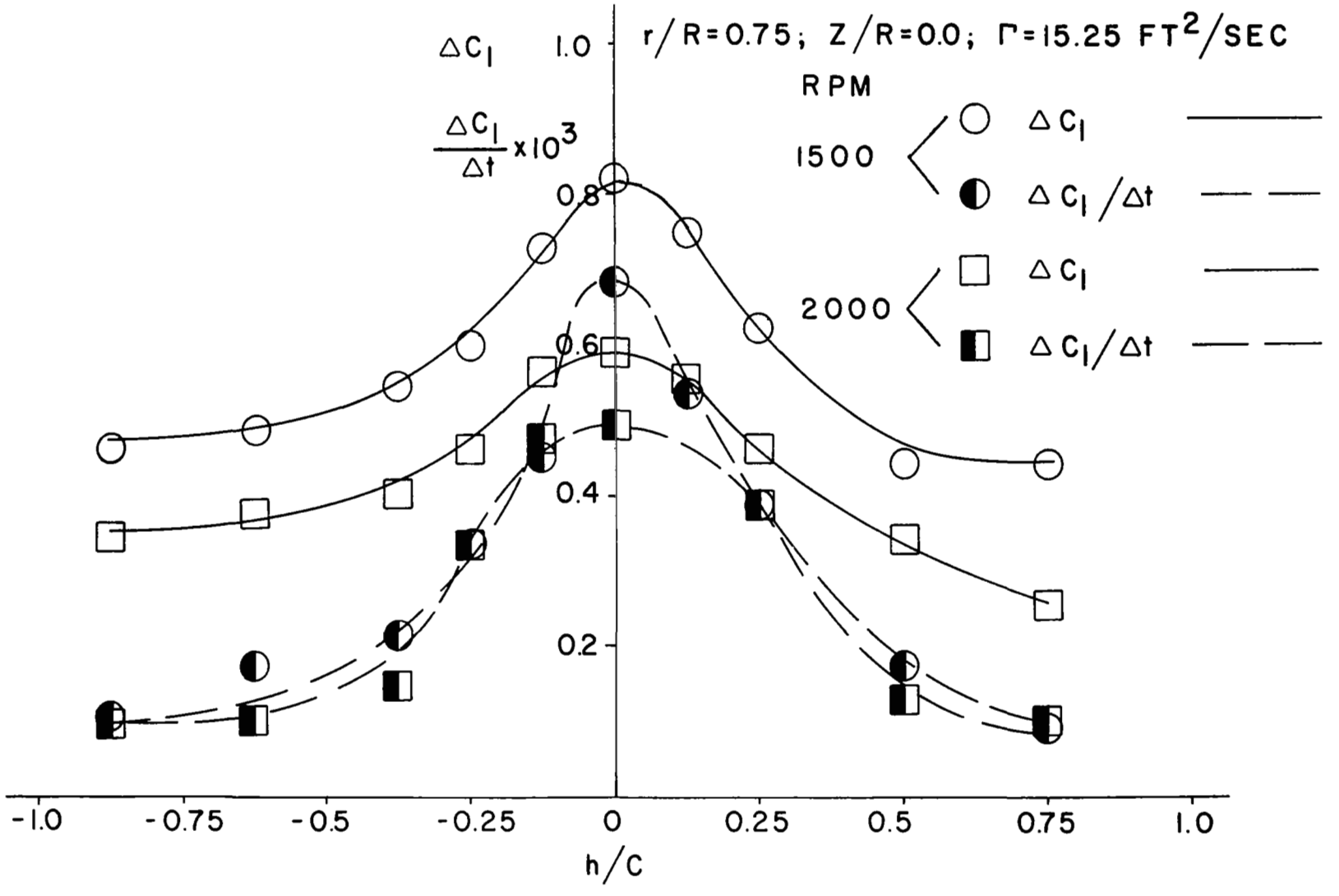

Fig. 16 Variation of ΔC_l and $\frac{\Delta C_l}{\Delta t}$ with Rotor Positions

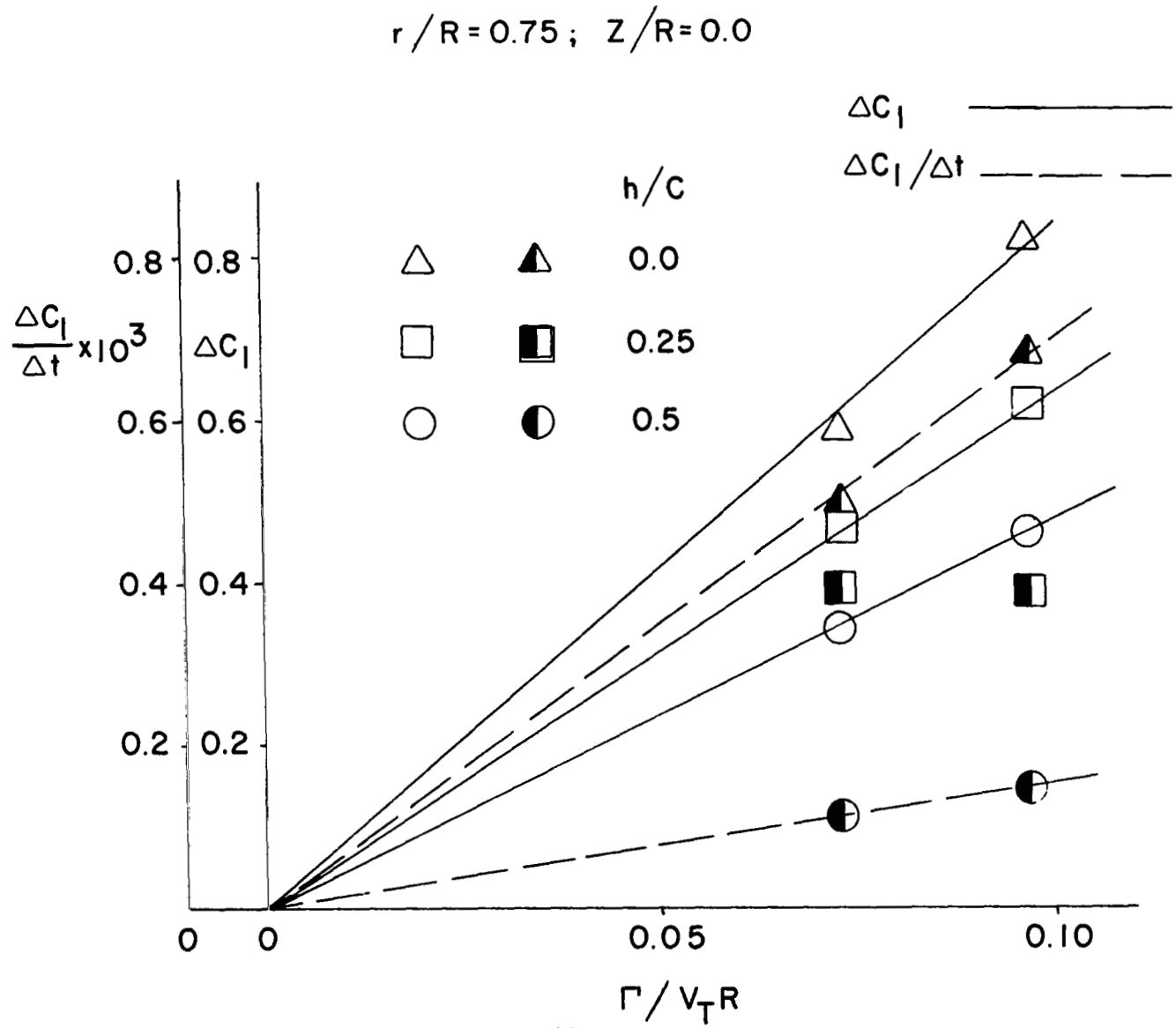

Fig. 17 Variation of ΔC_l and $\frac{\Delta C_l}{\Delta t}$ with Circulation

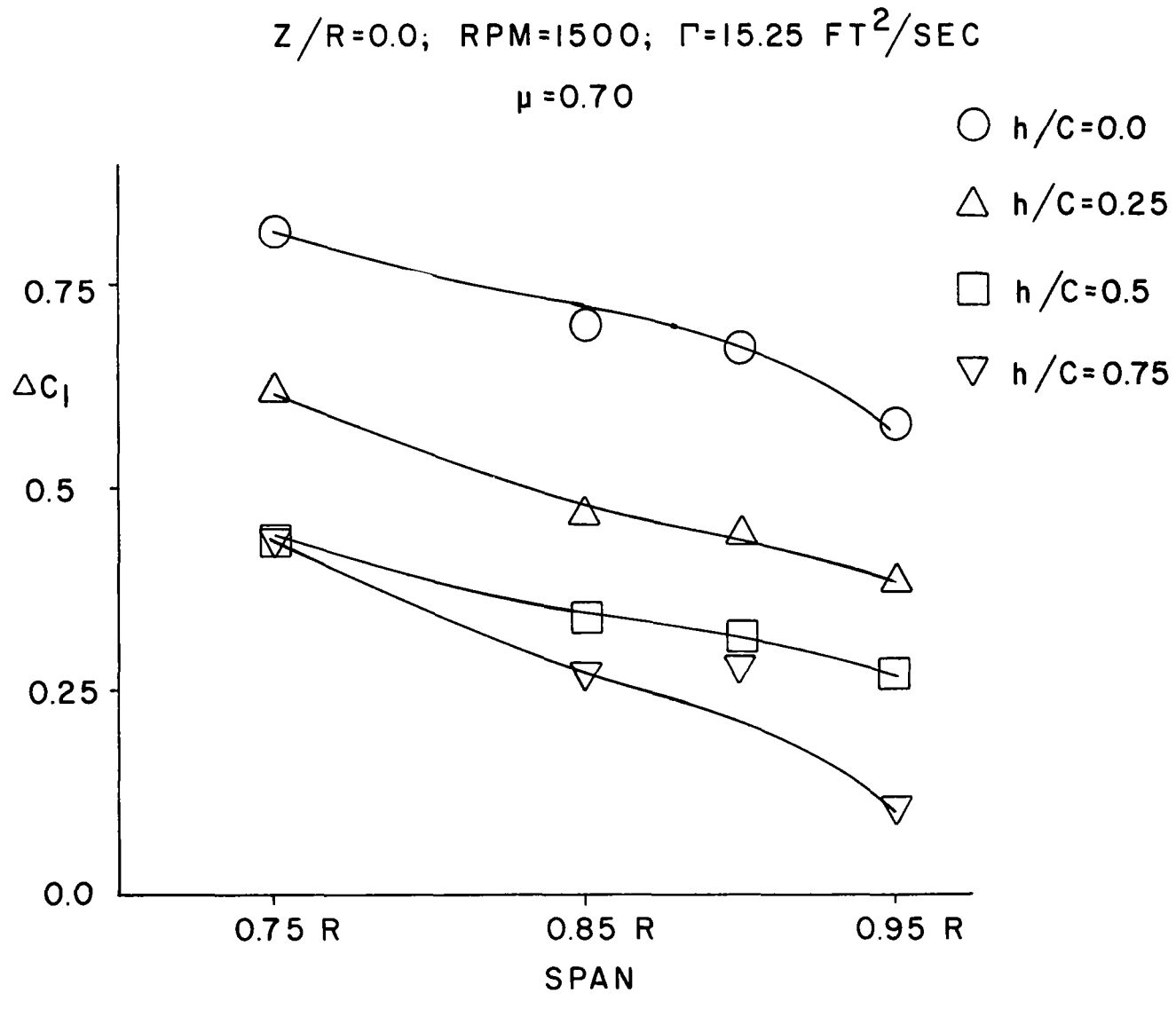

Fig. 18 Variation of ΔC_l with Span

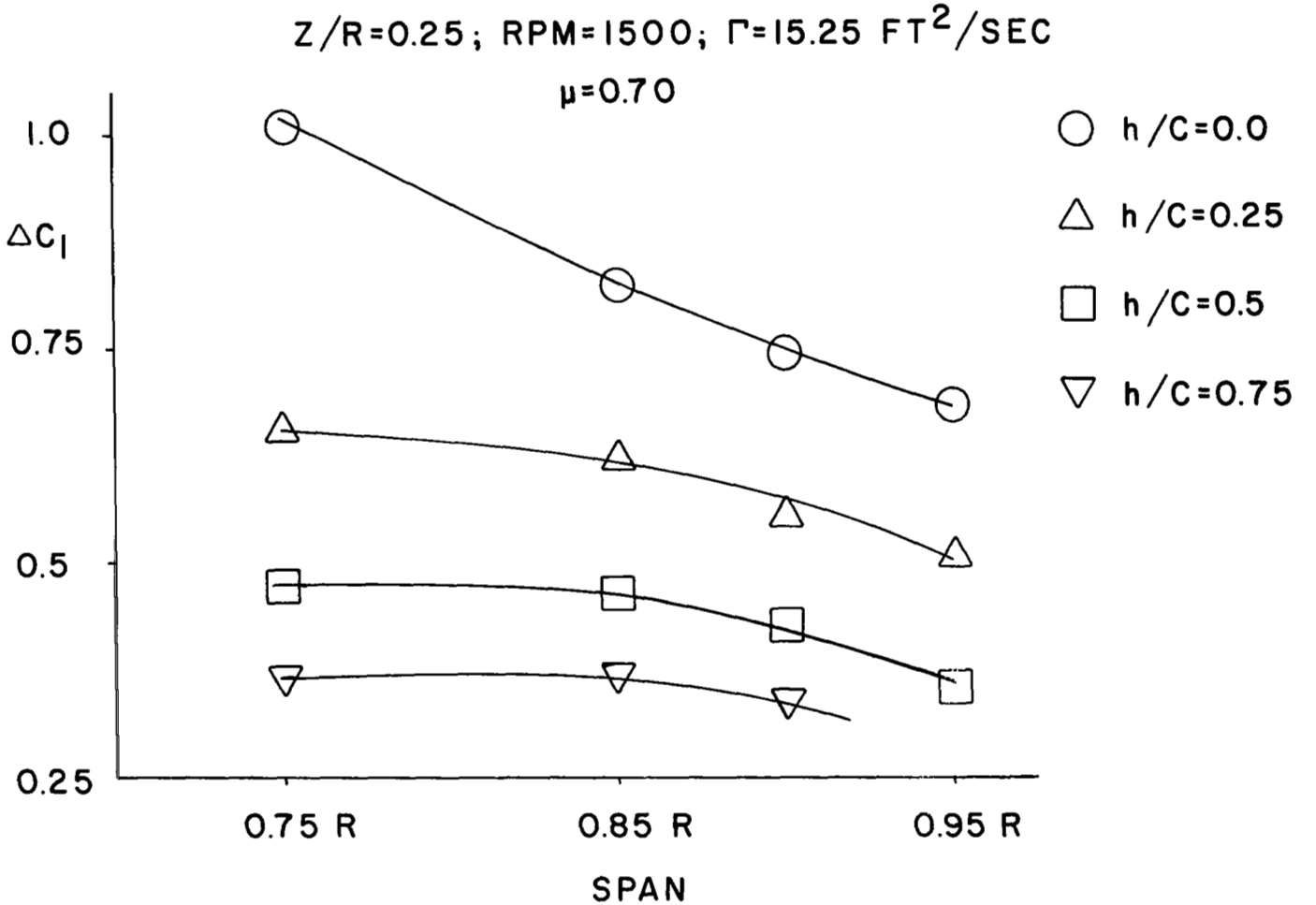

Fig. 19 Variation of ΔC_l with Span

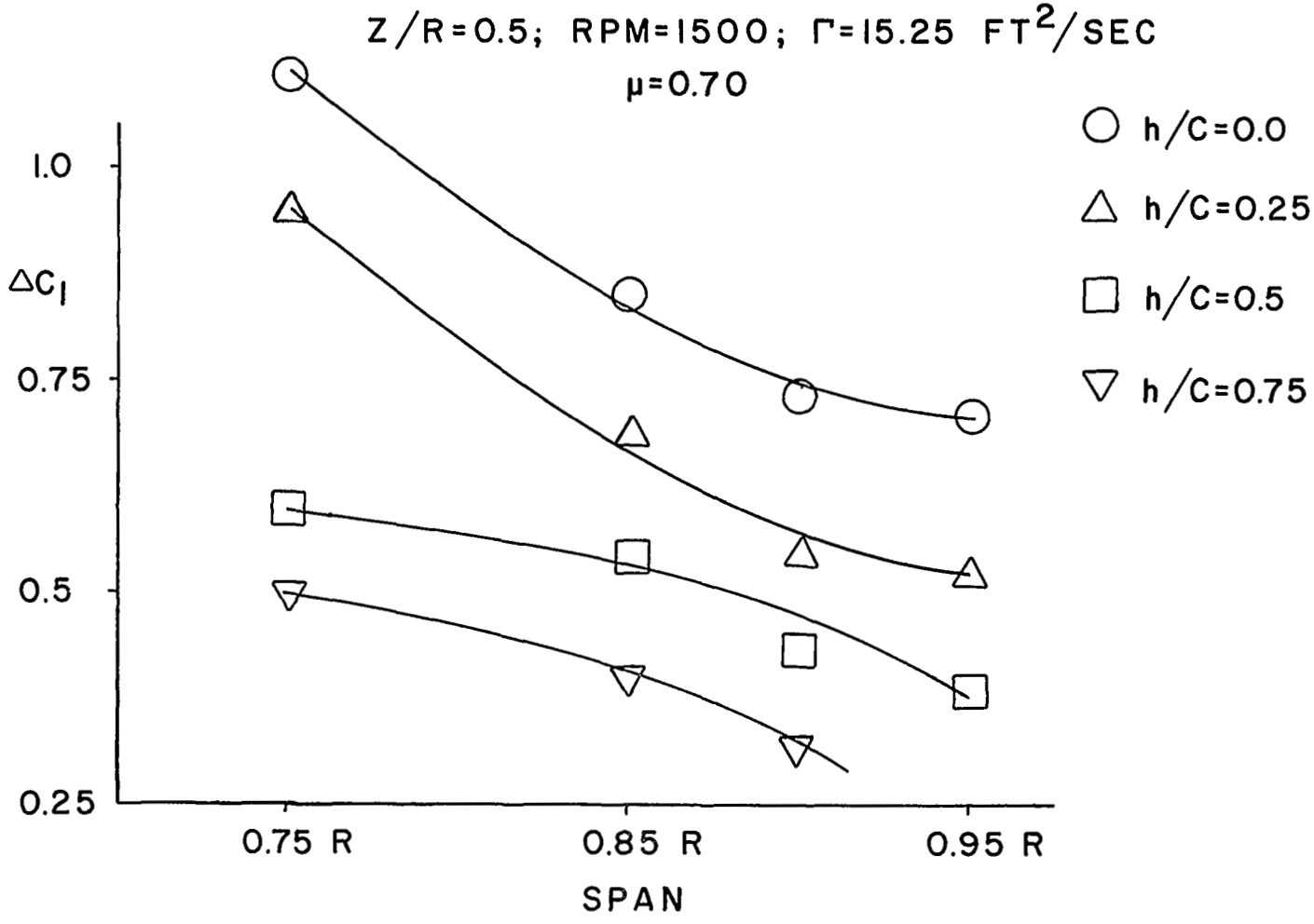

Fig. 20 Variation of ΔC_l with Span

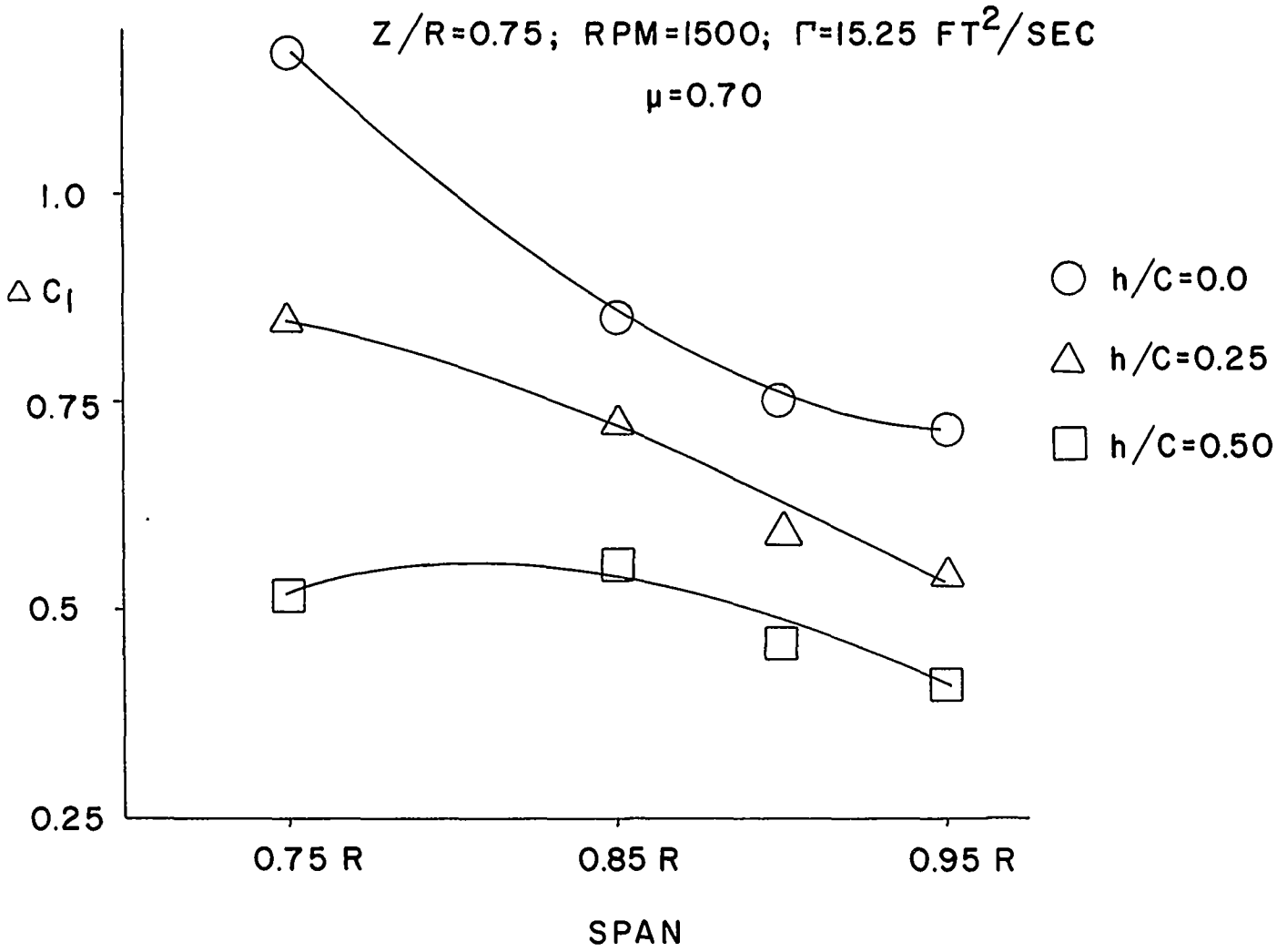

Fig. 21 Variation of ΔC_l with Span

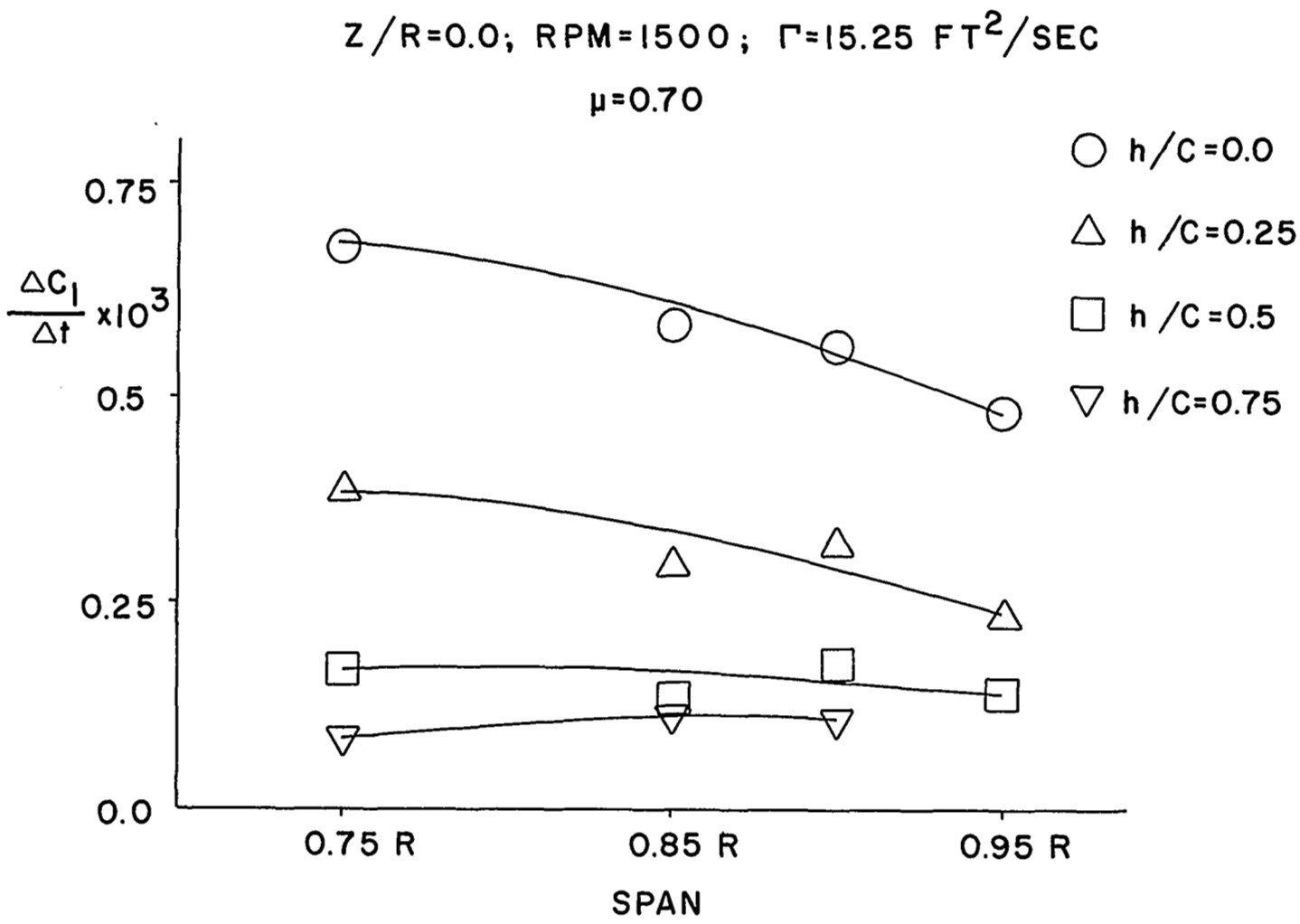

Fig. 22 Variation of $(\frac{\Delta C_l}{\Delta t})$ with span

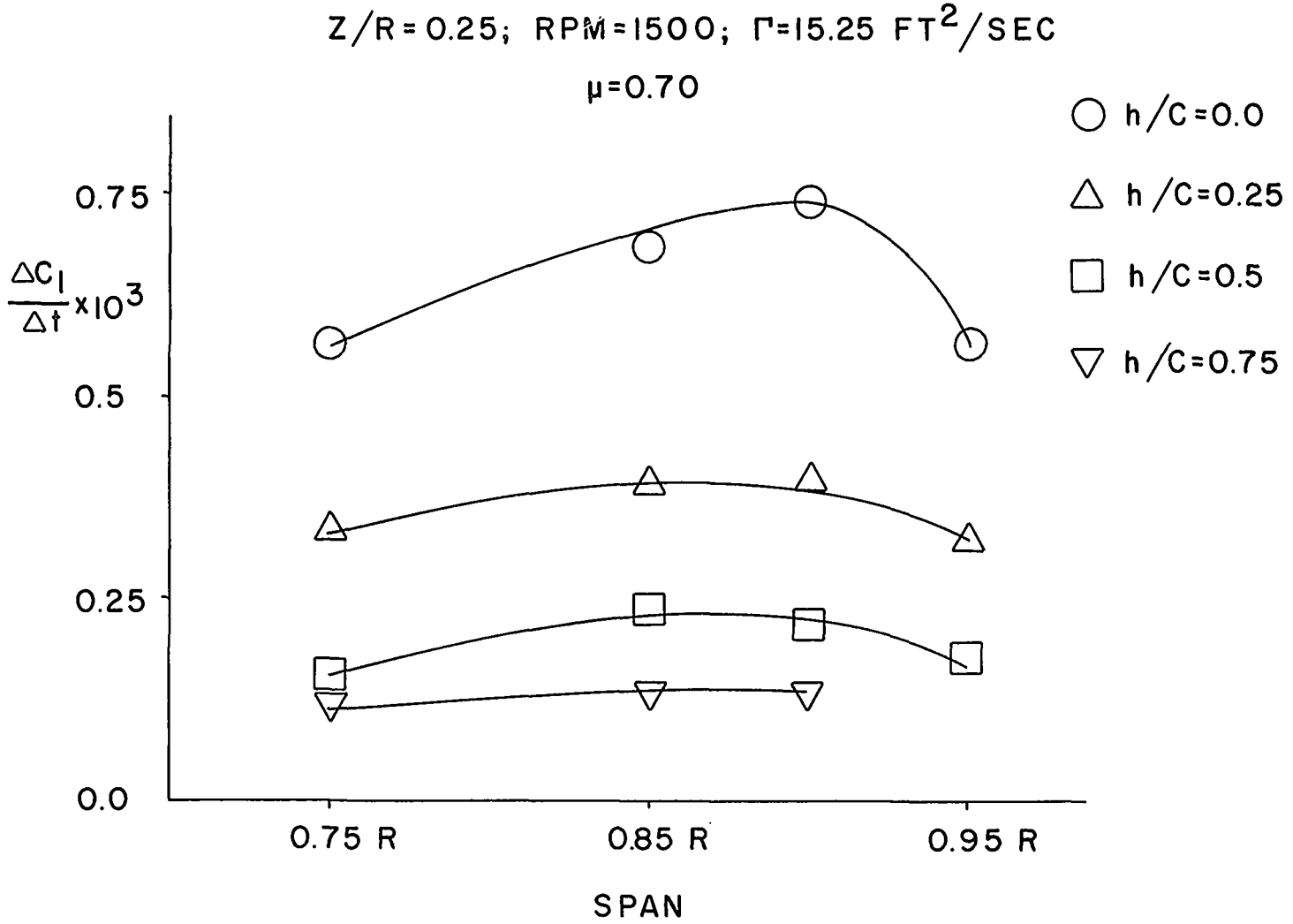

Fig. 23 Variation of $(\frac{\Delta C_l}{\Delta t})$ with Span

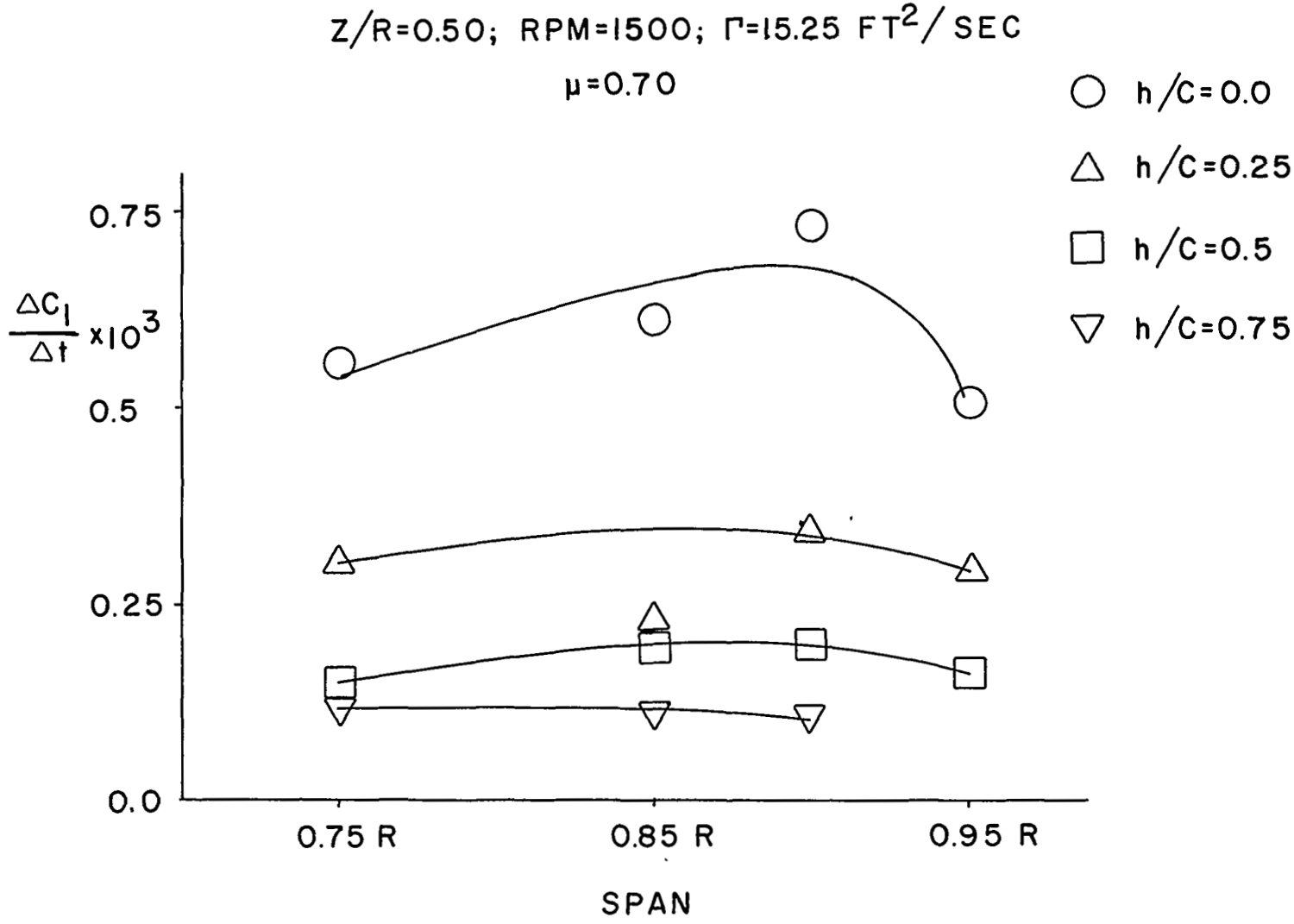

Fig. 24 Variation of $(\frac{\Delta C_l}{\Delta t})$ with Span

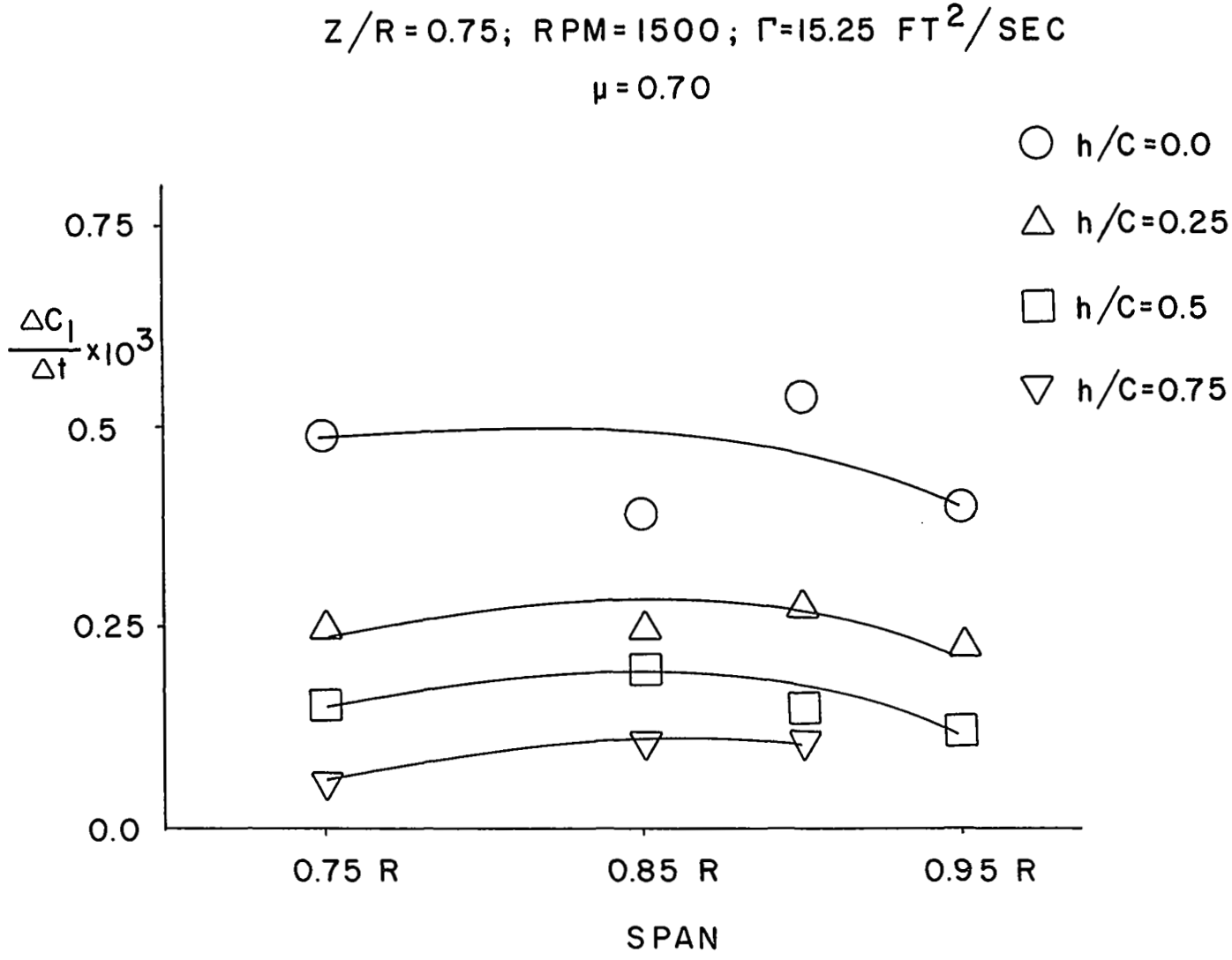

Fig. 25 Variation of $(\frac{\Delta C_l}{\Delta t})$ with Span

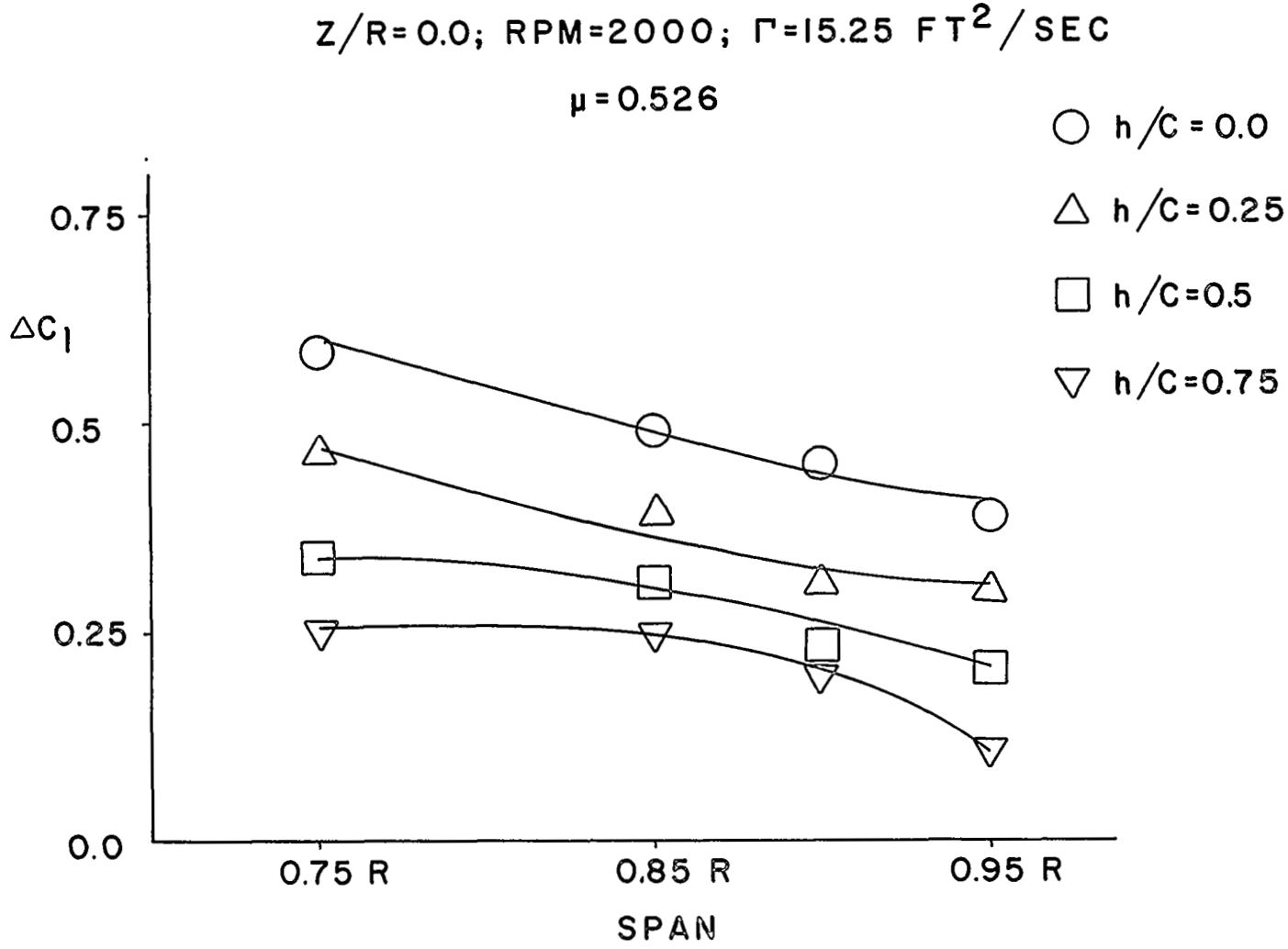

Fig. 26 Variation of ΔC_l with Span

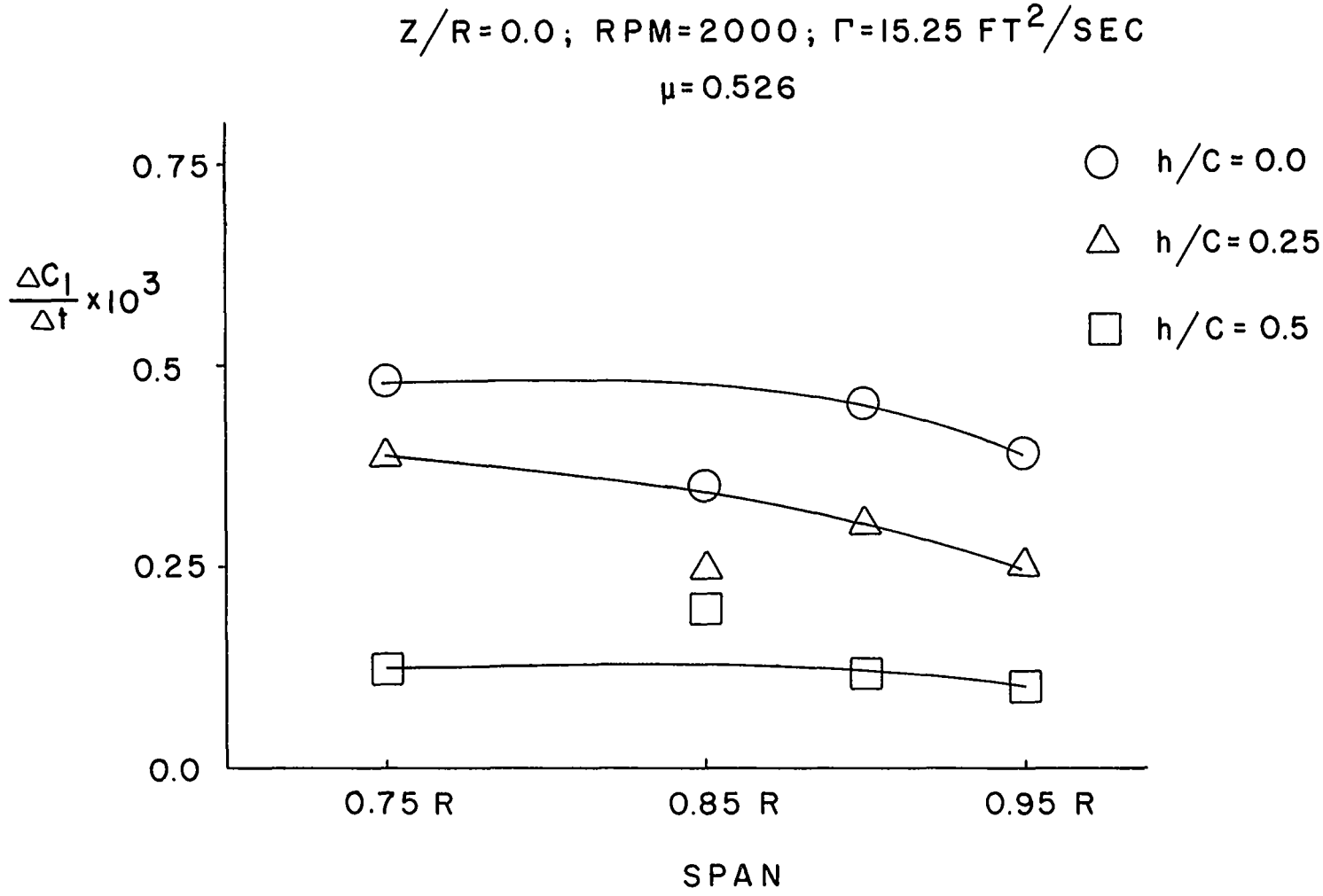

Fig. 27 Variation of $(\frac{\Delta C_1}{\Delta t})$ with Span

NASA-Langley, 1971 — 1 CR-1909